

Contents lists available at ScienceDirect

Cement and Concrete Composites

journal homepage: www.elsevier.com/locate/cemconcomp



Biochar-immobilized bacteria and superabsorbent polymers enable selfhealing of fiber-reinforced concrete after multiple damage cycles



Harn Wei Kua^a, Souradeep Gupta^{a,*}, Anastasia N. Aday^b, Wil V. Srubar III^{b,c}

- ^a Department of Building, School of Design and Environment, National University of Singapore, 4 Architecture Drive, (S) 117 566, Singapore
- b Materials Science and Engineering Program, University of Colorado Boulder, Boulder, CO, 80309-0428, USA
- ^c Department of Civil, Environmental, and Architectural Engineering, University of Colorado Boulder, Boulder, CO, 80309-0428, USA

ARTICLE INFO

Keywords: Self-healing Biochar Superabsorbent polymer Bacteria Fibers

ABSTRACT

Self-healing under multiple damage cycles is critical to the serviceability of concrete structures. This article explores crack closure and recovery of mechanical and permeability properties after multiple (i.e., three) damage cycles by comparing autogenous and bio-based self-healing in concrete using a combination of steel and PVA fibers, superabsorbent polymer (SAP), and bacteria immobilized in biochar. Swelling of SAP upon exposure to water and enhancement of hydration by curing action of SAP led to improved blocking and filling of cracks compared to a control (plain concrete); however, the effectiveness of autogenous crack closure (by only SAP or SAP plus fibers) was limited to narrow surface cracks (< 500 μm) after the third healing cycle. Microbial calcite precipitation by biochar-immobilized bacteria combined with SAP and fiber was found to offer superior closure for relatively wider surface cracks (> 600 µm) and internal micro-cracks compared to that attained by the autogenous mechanism alone in control and concrete containing only SAP and fiber. Effectiveness of crack filling by immobilized spores in biochar was found to be consistently higher than concrete with directly added spores and SAP through all three cycles of damage and healing. Precipitation of calcium carbonate crystals in internal cracks and interfacial zones around PVA fiber and aggregate in concrete with biochar immobilized spores resulted in high recovery of strength and permeability compared to the autogenous healing mechanism in control and concrete with SAP and fiber. However, it was found that macro-voids formed by SAP with a larger average particle size and higher swelling capacities affected total permeability and permeability recovery after repeated healing. Overall, we conclude that cementitious systems with biochar-immobilized bacteria, SAP, and fibers can enhance self-healing and impart improved durability to concrete structures.

1. Introduction

Building structures are often subjected to multiple cycles of loading that induce repeated damage to concrete. Unhealed cracks propagate over time and lead to further deterioration of concrete structures. Therefore, regardless of the technique selected, self-healing must be repeatable. In this work, self-healing refers to concrete's effectiveness in crack-closure and property recovery after multiple loading cycles [1]. Self-healing is a commercially attractive feature for concrete, given that high costs are incurred in repair activities to address several deterioration events throughout the service life of a concrete structure [2].

Some studies have previously investigated self-healing under multiple damage cycles using capsule-based approaches and autogenous healing mechanisms with superabsorbent polymers (SAPs) and PVA fibers, respectively [3–5]. Van Tittelboom et al. [3] tested the recovery

of strength and stiffness in concrete subjected to two damage cycles. Polyurethane (PU) was used as a healing agent, which was encapsulated in ceramic and borosilicate glass tubes within the concrete member. Cracks of width 400 μm were created using displacement-controlled loading. After the first loading cycle, the highest average recovery of strength was 61% for glass tubes, while, for the second cycle, recovery was reduced to 23%. Similar results were observed in the case of stiffness recovery, which were 64% and 34% for the first and second cycle, respectively. Thao [4] observed a similar recovery of stiffness for the first and second loading cycles of a reinforced concrete beam. In that study, isocyanate pre-polymer (epoxy) was encapsulated in glass tubes. Initial crack widths were maintained at $\approx 300\,\mu m$. A maximum of 88% and 85% of normalized stiffness recovery (expressed as the fraction of pre-damage stiffness) was observed for the first and second healing cycle of the concrete beams, respectively.

E-mail address: souradeepnus@gmail.com (S. Gupta).

^{*} Corresponding author.

Superabsorbent polymers (SAP) have been shown to improve selfhealing properties in cracks that occur in mortar and concrete via freeze-thaw cycles and autogenous shrinkage [6-8], making them an excellent candidate for self-healing approaches for concrete structures that undergo multiple damage cycles. SAPs are a class of crosslinked networks of hydrophilic polymers that absorb substantial amounts of water (10-100,000% by dry weight). Chemical and physical crosslinks render the polymer insoluble in solution, while ionic functional groups aid in the ability of the network to absorb solutions through ion-dipole interactions [9]. Snoeck et al. [5], for example, reported high recovery in strength by using a SAP in engineered cementitious composites. Samples with SAPs showed 75% and 66% recovery in strength after the first and second damage cycle, respectively, compared to 28% recovery in the case of the reference sample not containing SAP [5]. Wang et al. [8,10] proposed entrapping bacteria spores (Bacillus Spharicus) in modified alginate and chitosan-based pH responsive hydrogel (swelling capacity of 38-42 g/g in fluid of pH between 7 and 11, respectively) to generate self-healing of micro-cracks in cement mortar. However, 1% addition of modified alginate resulted in reduction of compressive and tensile strength of mortar by 20-30% compared to reference. Use of bacteria spores encapsulated in pH-responsive chitosan based hydrogel was found to be efficient in sealing crack width up to 400 µm and reducing water absorption by 81-90% compared to reference mix [8].

Additions of steel and polymer microfibers have proven effective in controlling crack widths in cementitious composites and have demonstrated increased self-healing efficiency [11,12]. Earlier research studies have reported that hybrid fiber combinations of polymer microfibers (e.g., PP and PVA fibers) and macro-fibers (e.g., steel fibers) offer improved composite action compared to the individual fiber-reinforced concrete. While short discrete fibers can resist propagation of microcracks, longer and tougher steel fibers can bridge macro-cracks and impart toughening mechanisms to the composite [13,14]. Moreover, PVA fibers act as nucleation sites for deposition of hydration products due to the presence of hydroxyl groups on its surface [12].

Immobilization of bacteria spores in porous fillers have also been found to improve self-healing efficiency of concrete [8,15]. Biochar, prepared by pyrolysis of wood waste, is one such admixture that can be used as an effective carrier for bacteria spores in cementitious materials [16]. Gupta et al. [16] found that spores of ureolytic bacteria (Bacillus Sphaericus) immobilized in biochar pores improved crack sealing and recovery of permeability of healed cement mortar. This concept is akin to application of biochar as a soil enhancer to improve plant growth by providing a shelter for rhizobium bacteria and other soil bacteria species [17,18] Using biochar as a carrier material in self-healing concrete would also facilitate sequestration of carbon in cementitious mixtures, while offering a new avenue for waste management. For instance, wood waste generated by local wood processing industries constitute a major fraction of disposed waste in Singapore [19]. Approximately 97,300 tonnes of wood waste was disposed in 2017. Bulk of the disposed waste is incinerated and landfilled at a site, 7 km off the cost of Singapore. Incineration and transport operations for landfilling leads to emission of particulate matters and release of greenhouse gases posing a challenge for a land constrained country like Singapore [20,21]. Therefore, producing biochar by pyrolysis of wood waste will divert a significant fraction of landfilled waste to value added product for the construction industry. It is estimated that depending on feedstock biochar has the potential to reduce greenhouse gas emission by 870 kg-CO2 equivalent of which 62-66% is realized from sequestration of stable carbon inherited from the biomass (feedstock) [22]. Therefore, pyrolysis of wood waste and application of wood based biochar in self-healing concrete may potentially lead to significant reduction in global anthropogenic emission by sequestering stable carbon in smart building and infra-

Together, studies on self-healing indicate that the desired performance of a concrete structure can be maintained using self-healing approaches that can recover strength, stiffness, and permeability after

repeated cycles of damage-inducing loading. Although some fragmented studies have been published on the effectiveness of multiple-cycle self-healing of concrete using polymeric agents, systematic investigations into the repeatability of self-healing using bio-based approach—for example, using calcium carbonate ($CaCO_3$)-precipitating bacteria—are limited. Thus, the aim of this work was to systematically investigate the efficacy of three self-healing approaches, namely bio-char-immobilized bacteria, SAP, and a combination of PVA and steel fibers, to heal concrete that has been exposed to multiple cycles of damage.

2. Materials and methods

2.1. Materials

Ordinary Portland cement conforming to ASTM C150 Type I was used for all mixes in this study. Locally available sand with maximum size 4 mm and size gradation conforming to ASTM C33 was used. Fineness modulus and specific gravity of the sand was 2.54 and 2.65, respectively. Coarse aggregate with maximum size of 19 mm was used. The oven-dry unit weight and water absorption capacity of coarse aggregates were 1650 kg/m³ and 0.80%, respectively.

Commercially available bacteria spores and bio-substrates – calcium nitrate, urea and yeast extract were obtained from Rely Chemicals Ltd., China. The culture procedure, media components and preparation of bio-substrates are proprietary information.

2.2. Biochar preparation and characterization

2.2.1. Preparation of biochar

Biochar was produced by pyrolysis of locally collected mixed-wood sawdust, which is a by-product of the wood milling industry. Sawdust was dried in an oven at 70–80 °C for 16 h before pyrolysis. Pyrolysis was carried out at 500 °C by heating the sawdust in a muffle furnace from room temperature (30 °C). A small vent and forced ventilation system provided with the furnace enabled the vapours to escape during pyrolysis in order to prevent re-deposition of organics and volatiles onto the biochar surface and pores. The heating rate was maintained at 10 °C/min until the pyrolysis temperature was reached. The temperature was then maintained for 60 min. The resulting biochar was allowed to cool to room temperature and stored in a sealed container.

2.2.2. Characterization of biochar

2.2.2.1. Particle size and morphology. The biochar was manually ground using a mortar and pestle. Particle size distribution (PSD) was determined by polarized intensity differential scattering (PIDS) using a laser diffraction particle size analyzer. 3–4 g of biochar was dispersed in water by mechanical stirring and laser beam was passed through the solution. The machine software (Beckman Coulter, LS13 320) calculated the size distribution (output) as volume equivalent of sphere diameter using the laser diffraction angle, which is influenced by particle size.

Structure and morphology of biochar particles was characterized by scanning electron microscopy (SEM) (JEOL JSM-6700F, accelerating voltage of $15\,\mathrm{kV}$). Dry biochar particles were coated with platinum using a magnetron sputtering coater (JEOL JFC-1600 auto-fine coater) before imaging.

 $2.2.2.2.\ Surface\ area,\ porosity,\ elemental\ composition,\ and\ water\ absorption\ capacity\ of\ biochar.$ Specific surface area (SSA) and pore volume of biochar was determined by employing multipoint N_2 adsorption using the Brunauer-Emmett-Teller (BET) method. Biochar samples were degassed over 8 h at 105 °C prior to BET. The t-plot method was used to determine the micro-pore surface area, while pore volume was calculated using Barrett-Joyner-Halenda (BJH) theory from desorption isotherm data.

Mercury intrusion porosimetry (MIP, AutoPore IV 9500) was used to estimate the average pore diameter of the produced char. This method was chosen because of its suitability to estimate dimension of pores over a wider size range (typically 0.01 μm –200 μm) compared to N_2 -BET [25]. Intrusion pressure was increased from 0.003 MPa to 130 MPa and the volume of intruded mercury was measured for each pressure increment.

Elemental composition of biochar was determined by electron dispersive spectroscopy (EDS) in combination with SEM. Multiple areas on the biochar particle surface were selected for sampling to estimate the carbon and oxygen content along with other trace metals that may be inherited from the feedstock of biochar.

Biochar particles tend to absorb and retain water due to their porous nature, which regulates the water content in biochar-supplemented cementitious systems. Water absorption capacity of biochar was determined using filtration method. $3-4\,\mathrm{g}$ (m_{db}) of oven-dry biochar was soaked in 80 g of water in a sealed glass beaker for 24 h. The water was then drained using a pre-wetted filter paper until there was no flow of free water from the beaker and all of the soaked biochar was collected in the wet filter paper. The mass of residual wet biochar and filter paper ($m_{w,bf}$) was measured and subtracted from the mass of pre-wetted filter paper (m_f) to calculate water absorption capacity (AC, g/g of dry biochar) using equation (1).

$$AC = \frac{m_{w,bf} - m_f}{m_{db}} \tag{1}$$

2.3. Fibers

Hybrid fibers composed of straight steel fibers and PVA fibers were used in this study. The properties of the fibers are presented in Table 1.

2.4. Superabsorbent polymers (SAP)

Two types of SAP were used in this study, namely a commercially available sodium polyacrylate based SAP (named 'SAP-A' henceforth) with a particle size 300 \pm 63 μm and a bio-based SAP with a particle size 450 \pm 57 μm (named 'SAP-B' henceforth). The bio-based SAP used in this study was synthesized in-house via free radical polymerization of acrylic acid and kappa carrageenan (κC). Carrageenans are a class of linear, hydrophilic polysaccharides present in various species of red seaweeds in the class, Rhodophyceae [26]. Synthesis methods for SAP-B have been previously reported by the authors elsewhere [26–29]. The radical initiator (ammonium persulfate, APS) thermally decomposes to produce a sulfate anion-radical. The radical can then abstract a hydrogen from the hydroxyl group of κC , creating an active center on the κC , which can then graft onto the acrylic acid backbone.

The swelling capacities of SAP-A and SAP-B, determined by the tea bag method [26] in deionized (DI) water, tap water, and cement filtrate, are presented in Table 2. Cement filtrate was made by adding 100 g of Type I/II cement to 1 L of deionized water. The solution was covered with parafilm and stirred at 400 rpm for 24 h before use. For each solution, three trials for absorption were conducted.

2.5. Mix design, mixing, and curing

2.5.1. Determination of biochar, SAP, and fiber dosage

The dosage of biochar (BC 500) used for immobilization of bacteria

spores was maintained at 1 wt% of cement, which was based on the influence of biochar at various dosages (0.50–2 wt% of cement at increment of 0.50%) on concrete strength and permeability [30]. 1 wt% of biochar addition was found to be optimal due to resultant improvement in strength and impermeability of concrete (data not shown). Bacteria spores (*Bacillus Sphaericus*) were immobilized in biochar by pre-soaking using a procedure described elsewhere [16].

Dosage of each SAP (A and B) was selected based on their respective effect on compressive strength and moisture retention capacity of mortar made with same water-cement ratio (w/c=0.40) as concrete mixes. 0.60% addition of SAP-A and SAP-B by weight of cement in mortar offered similar compressive strength as control samples under moist and dry curing conditions (see Table S1, Supplementary Information). Moisture retention in mortar with 0.60 wt% SAP was higher compared to other dosages (i.e., 0.30%, 1% and 2% by weight of cement). Therefore, 0.60 wt% SAP-A and SAP-B was selected to complement self-healing action in concrete mixes under repeated damage.

PVA and steel fibers were added at 0.30% and 0.20% by weight of cement, respectively. This proportion of steel and PVA fibers was found to sufficiently maintain integrity of concrete cylinders under three cycles of compressive loading (up to 70% of ultimate stress). Relatively low dosage of steel fiber was selected to minimize control fiber agglomeration and minimize the negative effect of steel fibers on concrete workability (Supplementary Table S4) [25]. Hybridization of PVA microfibers with steel fibers, produce an increase in strength and toughness beyond that can be achievable with steel fibers alone [14]. This is because the PVA fibers delay the formation of macrocracks by bridging and arresting micro-cracks, while steel fibers can resist propagation of macro-cracks. Due to higher specific bond energy and bond strength than steel fibers [31], PVA fibers do not get pulled out from matrix at low slip level and therefore, can delay coalescence of micro-cracks. Lawler et al. [31] reported that adding PVA fiber at similar or slightly higher dosage than steel fiber reduces spacing between fibers, which is effective in arresting micro-crack propagation and forms multiple narrow cracks instead of few wide cracks under loading. This modification in crack development is expected to contribute to durability since the water tightness and bacteria-based healing efficiency of the material is much improved if multiple cracking with controlled crack width takes place [14,32].

Although 60% loading level (in our study) results in stable crack formation and may not lead to macro-cracks after first cycle [33], some unhealed cracks would continue to grow and coalesce into macro-cracks under repeated damage cycles. Steel fibers are therefore necessary to maintain the integrity of samples after three damage cycles (in this study) by resisting uncontrolled macro-crack formation compared to control (plain concrete).

2.5.2. Mix composition

Table 2 shows the design proportions of the concrete mixes used in this study. Out of the eight mixes studied, plain concrete (PC (control) without any healing agent or fiber (PVA and steel) served as the control, while the other four mixes contained either only SAP (CON_SAP-A and CON_ SAP-B, respectively) or a combination of SAP and fiber (CON_SAP-A + Fib and CON_SAP-B + Fib). These mixes were considered, because SAP itself has been shown to impart self-healing effects, which would contribute to healing by bio-based agents [12]. Mix containing directly added spores with SAP and fibers was prepared, which will provide an evaluation of the contribution of biochar

Table 1
Physical properties of used steel and polyvinyl alcohol fiber (PVA).

Type of fiber	Length (mm)	Diameter (µm)	Elastic modulus (GPa)	Density (g/cc)
Straight steel fiber	20	160	200	7.90
PVA fiber	12	20	45	1.28

Table 2Mix composition of studied mixes.

Mix code	Cement (kg/m³)	Sand (kg/ m ³)	Coarse aggregates (kg/m ³)	Water (kg	g/m³)	BC500 (wt. % of —cement)	SAP (wt.% of cement)	Fiber (wt.% of t)	Bio-nutrients (wt.% of —cement)	Superplasticizer (wt. % of cement)
		111)	(kg/III)	Mixing water	Water in bio- nutrient and spore solution	-cement)		PVA	Steel	-cement)	
PC (control)	390	890	890	156		_	_	_	_	_	0.38
CON_SAP-A	390	890	890	156		_	0.60	_	_	_	0.51
CON_SAP-B	390	890	890	156		_	0.60	_	_	_	0.56
CON_SAP-A + Fib	390	890	890	156		_	0.60	0.30	0.20	_	0.57
CON_SAP-B + Fib	390	890	890	156		_	0.60	0.30	0.20	_	0.61
BS-direct + SAP A + Fib	390	890	890	132.85	23.15	_	0.60	0.30	0.20	12.35	0.56
(BS-BC)-SAP-A + Fib	390	890	890	132.85	23.15	1%	0.60	0.30	0.20	12.35	0.64
(BS-BC)-SAP-B + Fib	390	890	890	132.85	23.15	1%	0.60	0.30	0.20	12.35	0.69

immobilization on crack filling and recovery of properties. Finally, two mixes containing biochar-immobilized spores with SAP and fiber ((BS-BC)-SAP-A + Fib and (BS-BC)-SAP-B + Fib) were considered and evaluated for self-healing performance. Total water-cement ratio was maintained at 0.40 for all mixes. No additional water was used for mixes containing SAP, because increased amount of internal free water in the matrix at early ages would also influence self-healing by enhancing hydration. These proportions are similar to the mix designs proposed in earlier studies [12,34], where a constant water-binder ratio was used for concrete containing SAP.

Bio-nutrients comprised of yeast extract, urea, and calcium nitrate were added at 0.35%, 4% and 8% by of weight of cement, respectively. Spore solution was added at 3.50% by weight of cement in concrete. The concentration of bacteria (Bacillus Sphaericus) was 10^{10} CFU/ml of the solution. Amount of mixing water was adjusted for the moisture in calcium nitrate (Ca(NO₃)₂.4H₂O) and spore solution. Ca(NO₃)₂.4H₂O contains 30.50% water. Therefore, mixing water was reduced by $(0.305\times0.08~x~390)\approx9.50~kg/m^3$ water contained in Ca(NO₃)₂.4H₂O (added at 8 wt% of cement) and $(0.035\times390)\approx13.65~kg/m^3$ of water in spore solution.

The dry components (i.e., cement, aggregates (coarse and fine), SAP, and yeast extract (where applicable)) were dry-mixed first for 1–2 min. Superplasticizer and bio-nutrients, including calcium nitrate and urea, were dissolved in mixing water by slowly adding them over the next 40–50 s. Mixing continued for 3–4 min until a homogeneous mix was achieved. Fibers (steel and PVA) and biochar-immobilized spores were then added. Finally, mixing continued for another 3 min. The fresh mix was cast into cylinder molds (100 mm(d) x 200 mm(h)) and placed on a vibration table for sufficient compaction. Fresh concrete was cast in 4 layers. Each layer was vibrated for 10–15 s until no air bubble on the surface was visible. The cast concrete mixes were covered with polythene sheets and stored in a laboratory environment (26–30 °C, 70–80% RH). Samples were demolded after 24 h and stored in a fog room (26 °C, 100% RH) for curing.

2.6. Methodology

Healing over three damage/healing cycles was investigated in this study. After 14-days of curing in a fog room, concrete samples were damaged by compressive loading to 60% of the peak load carrying capacity (60% f) of respective mixes. The selection of this damage level (60% f) is based on the failure mechanism of concrete involving microcrack initiation, stable growth, and propagation until the cracks coalesce leading to failure. These correspond to 30% f, 50–60% f and 100% f, respectively, according to the quasi-linear constitutive relationship between stress and strain for concrete under compression [33,35]. Therefore, 60% f would contribute to non-linear and inelastic deformations in the form of stable micro-cracks that would significantly affect permeability and mechanical behavior of the damaged concrete.

The damaged samples were allowed to heal in a fog room for the next 14-days before being tested for mechanical strength, elastic modulus, and permeability. Recovery of original properties at each cycle of healing is determined by comparing properties of healed sample with that of undamaged samples for a mix at the same time period. For example, after the first cycle of healing, the mechanical and permeability properties of healed concrete were compared with the 28-day properties of an undamaged mix to determine the recovery of original properties post-healing.

At 28-days, healed samples were again loaded at 60% of the undamaged peak strength to inflict damage for the second cycle of healing. After 14 days of healing, strength and permeability properties were compared with the 42-day properties of undamaged concrete of the same mix. A similar procedure was followed for the third cycle of healing.

2.7. Test methods

2.7.1. Mechanical and permeability tests

Compressive strength and elastic modulus of healed and undamaged samples were measured according to ASTM C39 [36] and ASTM C469 [37], respectively. The casting face of the cylinders were made smooth and level by wet grinding to facilitate uniform displacement and loading during testing.

Capillary absorption and sorptivity behavior of samples were investigated to quantify recovery in permeability after healing. Although micro-cracks may not significantly affect mechanical performance, water absorption of cement-based materials is sensitive to presence of pores and micro-cracks, which increase open porosity of the matrix. Capillary absorption and sorptivity was conducted according to ASTM C1585 [38] using $100\,\mathrm{mm}\,(\mathrm{d}) \times 50\,\mathrm{mm}\,(\mathrm{h})$ samples, that were wet-cut from cylinder specimen by a high-speed concrete cutter. The samples were conditioned as per the testing standard [38], and the side surfaces were coated with epoxy to ensure unidirectional transport of moisture through capillary suction from the submerged face.

2.7.2. Measurement of crack filling

During the healing period, filling of surface cracks was monitored using an optical microscope (Olympus SZX10, Olympus Corporation, Japan) fitted with a Leica illumination system. Some of the samples were loaded to complete failure after each cycle. Since the regain in properties after complete failure was minimal, these samples were used to visualize crack closure. For monitoring of crack closure, samples were subject to wet-dry cycles that consisted of approximately 9 h of wetting in fog room followed by 15 h of dry external conditions each day to simulate climatic conditions in tropical regions, which is characterized by high humidity, warm temperatures, and frequent rain.

The crack filling was calculated as the percentage (%) of initial crack width (created immediately after loading) that was sealed during

the 14-day healing period after each cycle. The visual filling of cracks served to qualitatively measure the healing capacity by autogenous mechanisms (for example, triggered by SAP) and bacteria-generated carbonate precipitation.

2.7.3. Thermogravimetric analysis

Thermogravimetric analysis (TGA) was conducted to estimate the distribution of hydration products in cement paste containing 0.60 wt% SAP-A and SAP-B respectively (water-cement ratio of 0.40), subject to moist and dry curing. A control paste was also prepared with the same water-cement ratio for comparison. 30–35 mg (M_cp) of ground samples (passing 106 µm sieve) were weighed and then allowed to thermally decompose in a thermogravimetric analyzer (Shimadzu, DTG-60) between 30 °C and 950 °C with ramping rate of 10 °C/minute.

Calcium hydroxide (CH,%) is estimated from the mass loss between 420 °C and 540 °C due to thermal decomposition of cement paste [39]:

$$CH loss (\%) = 4.12 \times (M_{540} - M_{420})/M_{cp}$$
 (2)

Where, M_{540} and M_{420} refers to loss in mass of cement paste at 540 °C and 420 °C respectively.

3. Results and discussion

3.1. Characterization of produced biochar

3.1.1. Particle size and morphology of biochar

The overall size of manually ground biochar (BC500) ranged from $2\,\mu m$ to $100\,\mu m$, with d_{50} and d_{90} of $9.92\,\mu m$ and $31\,\mu m$ respectively (Fig. 1). PSD of cement used in this study was also determined using the same laser diffraction method and presented in Fig. 1. A significant fraction (about 90%) of biochar particles were finer than the cement used in this study.

A SEM micrograph of biochar particles, shown in Fig. 2, confirmed the existence of macro-pores of 10– $20\,\mu m$ on the surface of biochar particles. The particles have a rough surface and fibrous morphology, which is typical of wood based biochar [40].

3.1.2. Surface area, elemental composition and water absorption capacity of produced char

The BET surface area of the biochar was $196.92\,m^2/g,$ while the micro-pore area and BJH pore volume were $140.88\,m^2/g$ and $0.0123\,cm^3/g$ respectively. The results show that micro-pore surface area contributes to about 70% of total BET surface area. The average pore diameter of biochar from mercury intrusion porosimetry was found to be $3.80\,\mu m.$

The carbon and oxygen content of biochar was $87.13 \pm 1.77\%$, $7.21 \pm 1.50\%$ respectively along with trace amount of other elements,

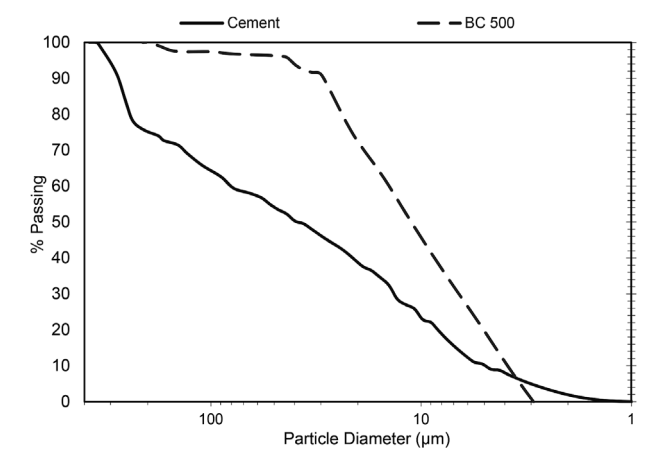


Fig. 1. Particle size distribution of biochar (BC 500) and cement grains.

including silica (0.40–0.45%), calcium (0.26–0.65%), aluminum (1.05–1.35%), potassium (0.40–0.50%) and magnesium (0.51–0.58%).

The water absorption capacity expressed as the mass of absorbed water per gram of dry biochar from three trials was $4.50\pm0.70\,\mathrm{g/g}$, which includes both free and bound water within in the biochar particles.

3.2. Swelling capacity of SAPs

Table 3 shows that swelling capacity of both SAP-A (polyacrylate based) and SAP-B (bio-based) are affected by increase in pH of the absorbate liquid. It is evident that presence of mono and divalent cations (Ca^{2+} , Na^+ , K^+) reduce swelling capacity of SAP-A and SAP-B, which is attributed to electrostatic attraction of cations towards anionic functional groups in the polymer network of the SAPs [28]. One can observe that SAP-B show 160% and 200% increase in fluid absorption in deionized water and tap water compared to SAP-A, while the difference in absorption of cement filtrate by SAP-B and SAP-A is statistically significant. Although larger particle size of SAP-B compared to SAP-A is an influencing factor for higher absorption, previous studies have reported that natural ability of kappa-Carrageenan (κ -C) to form gels in presence of cations lead to higher absorption of bio-based SAP s compared to acrylate based (non-bio-based) SAPs [26,41].

3.3. Effect of SAP and immobilized bacteria on crack filling

Fig. 3 shows the filling and closure (%) of cracks with respect to the range of initial crack widths after the first, second, and third cycles of loading. Width of cracks, created by compressive loading, varied between 200 and 800 μm , although some wider segment of cracks between 800 μm and 1 mm were observed in plain concrete (control) and mixes with only SAP-A and SAP-B. Plain concrete shows approximately 81% closure of narrow surface cracks (below 200 μm) in first cycle, although this decreases to 35% and 40% upon the second and third healing cycle, respectively. Minimal closure was observed for cracks beyond 400 μm width. Presence of SAP-A and SAP-B improved sealing of cracks (30–50% sealing ratio for wider cracks between 300 and 550 μm) compared to only 12–30% for the control after the first cycle. The combination of SAP with fiber also contributed to efficient closure of cracks, showing 30–60% sealing of crack widths between 300 and

A comparison of healing across different cycles show that SAP or combination of SAP and fiber yield consistently higher closure for cracks up to 400 µm compared to plain concrete. For example, in the range of 300–400 μm width of cracks, CON_SAP A + Fib showed 60% sealing after first cycle, while it was 55% and 43% in case of second and third cycle respectively. On the contrary, plain concrete showed 30%, 0%, and 5% sealing in similar range of crack width after the first, second, and third cycle, respectively. Superior performance of SAPcontaining mixes is attributed to the effects of SAP in assisting hydration and carbonate precipitation near the crack tip under wet-dry external condition [5]. During wet-cycle, sufficient moisture is available, which can be absorbed and retained by SAP particles. The absorbed moisture in SAP (A and B) can be made available for continuing cement hydration under dry external condition. TGA results confirm that cement paste with SAP-A and SAP-B generated 3.80% and 3.20% more CH respectively compared to control paste under dry external condition (Table S2, Supplementary Information), which indicates improvement in hydration due to self-curing action of SAP. This contributes to autogenous sealing of cracks, depending on distribution of SAP near the cracked site. Although sufficient moisture is present during wet curing periods, plain concrete fails to retain moisture effectively, unlike SAPcontaining mixes, thereby exhibiting lower closure ratios. SAP particles also retain the calcium-rich fluid, which would otherwise be washed out from the crack face. This provides the possibility of calcium carbonate generation at the crack tip [5,12], which has been found to seal

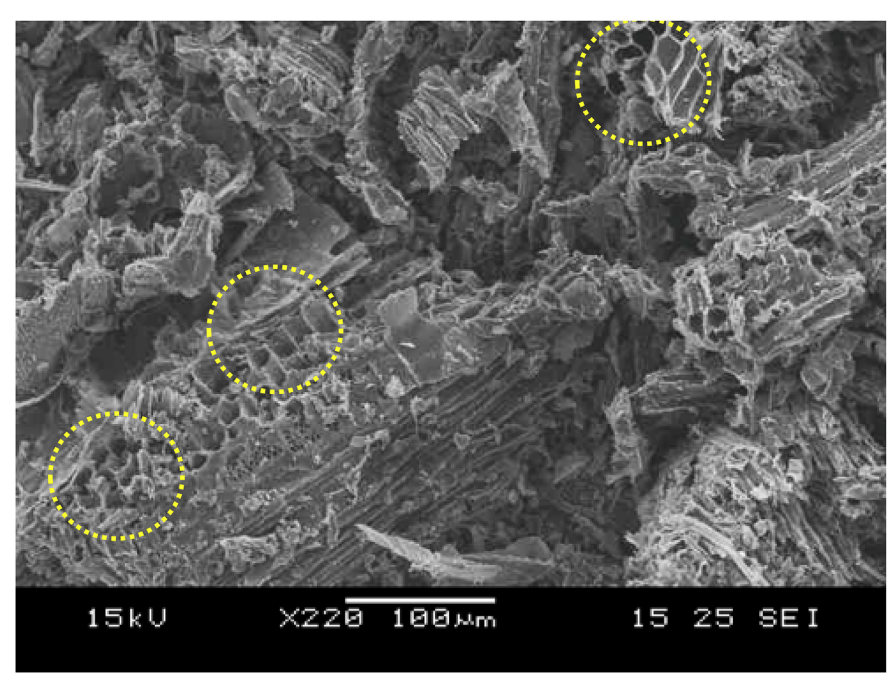


Fig. 2. SEM micrograph of biochar particles.

Table 3
Maximum swelling capacity (g/g of dry SAP) of SAP-A and SAP-B in solutions of different pH.

	Deionized water (pH ≈ 7.05)	Tap water (pH ≈ 7.80–8.09)	Cement filtrate/synthetic pore solution (pH >12.50)
SAP-A	$120.23 \pm 4.45 321.73 \pm 23.08$	65.69 ± 2.65	20.85 ± 4.22
SAP-B		300.34 ± 8.96	33.74 ± 4.73

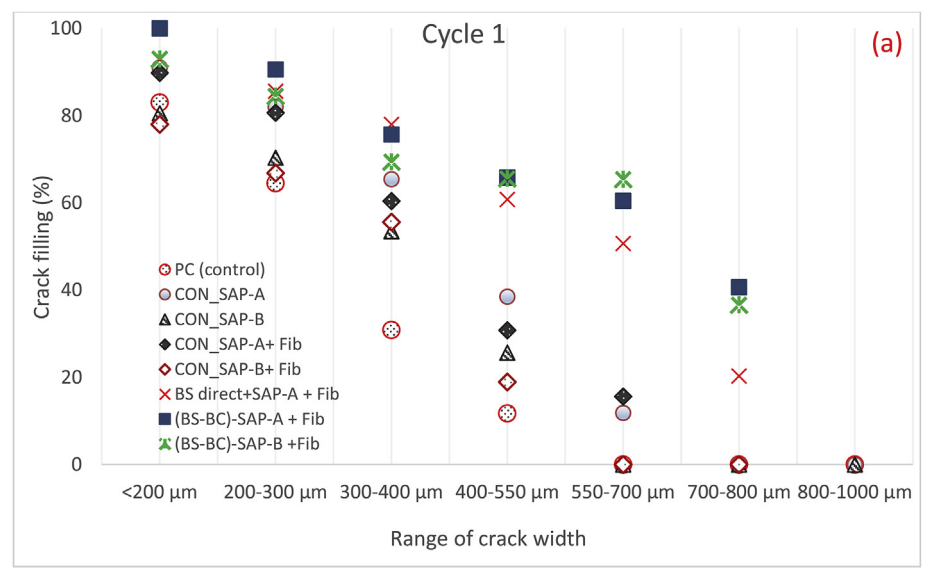
relatively wide micro-cracks in the range of 300–450 μm (Fig. 4(a)). Microscopic images also revealed wrapping of calcium carbonate crystals around the PVA fibers (Fig. 4(c)). Hydrophilic surface of PVA fiber provides anchorage and nucleation site for calcite crystals [12], that can efficiently bridge across the crack (Fig. 4(a)). However, wider cracks (about 680 μm) could not be filled completely by action of SAP and fiber.

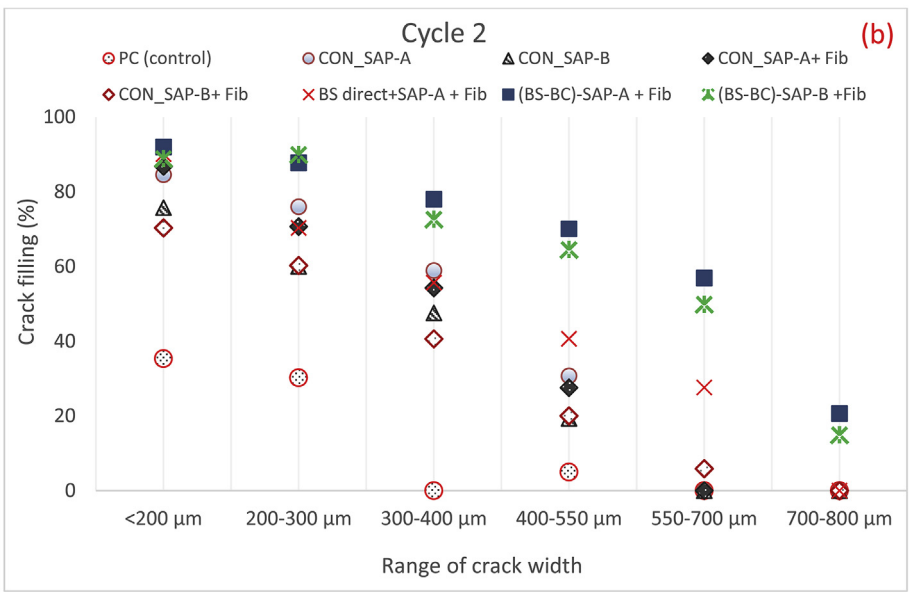
However, mixes with SAP-B showed slightly lower crack closure compared to mixes with SAP-A, especially for wide initial cracks. For example, for narrow cracks (< 200 µm), CON_SAP-A and CON_SAP-B show similar closure ratio (%), while, for cracks in the range of 300-400 μm and 400-550 μm, CON_SAP-A show 65% and 39% closure, respectively, compared to 53% and 26% closure exhibited by CON_SAP-B after the first damage-healing cycle. This result may be attributed to the higher swelling capacity and larger particle size of SAP-B compared to SAP-A, resulting in the hydrogel expanding out of the wide cracks and pores on the sample surface (Fig. 4(d)). This is confirmed from SEM image of the swelled gel (Fig. 4(e)), collected from the surface of the concrete samples. EDX analysis showed that carbon (78.95 \pm 4.73%) and oxygen (18.74 \pm 4.01%) are the main constituents of the gel, which is due to presence of acid groups (- COOH) and carboxylate salts (COO⁻) in the partially neutralized bio-based SAP (SAP-B in this case) [26]. Trace amount of calcium (1.44 \pm 0.20%), $(0.12 \pm 0.06\%)$ and aluminum $(0.28 \pm 0.12\%)$ were detected, which is probably due to the mixing of binder phase from cement hydration (calcium silicate hydrate and calcium aluminate hydrate) during collection of SAP gel from the concrete surface. Further SEM micrographs and EDX analysis on the swelled SAP-B, dry SAP-B and calcium carbonate (collected from healed concrete cracks) are presented in supplementary information (Fig. S4). Some of the swelled SAP s (SAP-B) tend to be detached from the concrete surface, which lowers its effectiveness in generation of carbonate and autogenous sealing product at the crack face under dry external environment.

The combination of biochar-immobilized bacteria, SAP, and fiber show appreciable crack filling in the range of 60–85% for cracks up to $550\,\mu m$ wide. The efficiency of crack filling in biochar immobilized bacteria concrete is higher than mix containing SAP (or combination of SAP and fiber), which is evident from significantly higher crack filling ratio (about 30–60% higher) for 400–800 μm wide cracks after cycle 1, cycle 2 and cycle 3 (Fig. 3). Although it is difficult to segregate the contribution to crack filling by SAP and biochar immobilized bacteria respectively in (BS-BC)-SAP-(A or B) + Fib samples, the results clearly suggest that generation biogenic calcium carbonate has significantly improved the crack filling effectiveness of this material combination (biochar immobilized bacteria with SAP and fiber) compared to concrete with only SAP and fiber. Precipitation of bio-calcite boosted filling efficiency especially in case of wide cracks.

However, beyond 550 μm , there is a reduction in closure capacity with biochar-immobilized spores, although the closure is improved compared to samples with directly added spores. The difference is more prominent after cycle 2 and cycle 3. For instance, for crack widths in the range of 550–700 μm , (BS-BC)-SAP A + Fib showed filling of 60%, 56% and 41% after cycle 1, cycle 2 and cycle 3, respectively, compared to 51%, 28% and 19% for the BS direct+SAP A + Fib mix. Similar trend is found for narrower cracks (400–550 μm), where biochar immobilization resulted in lower reduction of crack sealing effectiveness over the three tested cycles. Lower reduction in sealing effectiveness indicates the role of biochar immobilization in maintaining self-healing activity over multiple damage cycles (three in this case).

Fig. 5(a) and (b) show that the combination of biochar-immobilized spores and SAP A and SAP B completely sealed some surface cracks on the damaged concrete samples during the third healing cycle. The widest segment of the closed cracks in Fig. 5(a) and (b) was $676 \mu m$ and $800 \mu m$ respectively. Internal sealing of cracks was also observed by





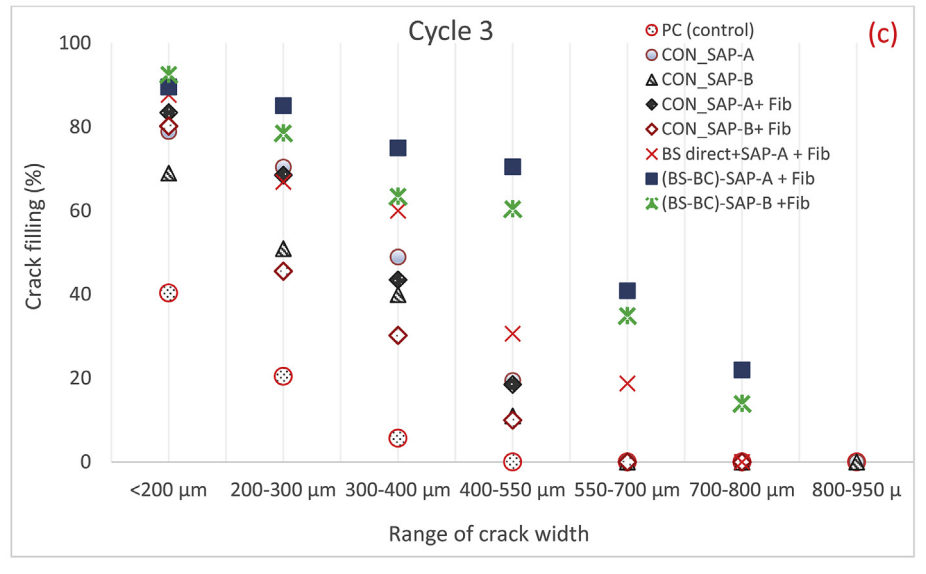


Fig. 3. Crack filling after (a) 1st, (b) 2nd, and (c) 3rd cycle of healing.

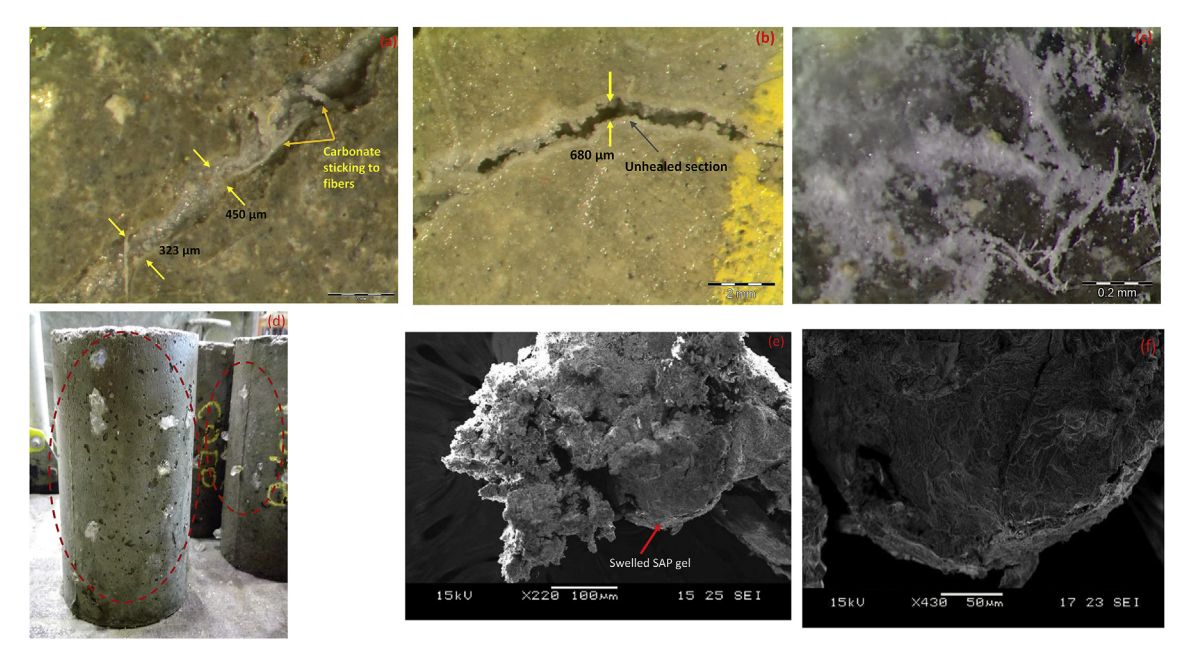


Fig. 4. (a) Carbonate precipitation at the crack face with SAP-A and hybrid fiber (b) unhealed section of wider crack in concrete with SAP-A and fiber (c) Wrapping of calcium carbonate crystals around PVA micro-fibers (d) SAP-B gels expanding through cracks and pores on the concrete surface (highlighted in red). (e) SEM image of the swelled gel, collected from concrete surface (f) Magnified image of swelled SAP-B gel, collected from concrete surface. (For interpretation of the references to colour in this figure legend, the reader is referred to the Web version of this article.)

breaking the damaged samples near the location of cracked sites on the surface. Fig. 5(c) and (d1) shows that internal cracks of width 450–700 µm were completely sealed by whitish precipitate. Fig. 5 (d2) confirm that the precipitate, collected from crack face, consist of rhombohedral crystals (calcium \approx 46 wt%, carbon \approx 29 wt% and oxygen \approx 25 wt%), which is typical of calcite produced by bacterial metabolism [32]. Similarly, in case of (BS-BC) -SAP-A + Fib, complete filling of surface crack of width 680 µm and 798 µm can be observed (Fig. 5 (e1)). SEM micrograph of the whitish precipitate collected from the crack site shows presence of calcium carbonate crystals around a germinated cell (rod-like) of Bacillus Sphaericus (Fig. 5(e2)), confirming generation of bio-calcite leading to crack sealing.

Partial closure of cracks was also observed at a few locations within the concrete samples containing biochar-immobilized bacteria and SAP (A and B). For instance, Fig. 5(f) shows limited closure of a crack passing through coarse aggregates in (BS-BC)-SAP-A + Fib, although the extension of the same crack is likely sealed by autogenous mechanism. Sealing of cracks need the presence of a healing agent or Ca²⁺, neither of which can be provided by the aggregate particles. Similar observation was made by Snoeck and De Belie [5], who reported limited sealing by hydration around sand particles in mortar containing SAP as a healing agent. Fig. 5 (g) shows that, although a 560 µm-wide part of a crack within the (BS-BC)-SAP-B + Fib paste was sealed by carbonate, some portions of the same crack (between 300 and 400 μm) were unsealed. This result is attributable to insufficient carbonate generation at the crack site, which may be linked to reduced bacterial activity and conditions at the crack site itself. In the event of surface cracking, some calcium ions leach out, which react with dissolved carbon dioxide to form carbonate at the crack face [5,12]. Therefore, surface cracks are closed more completely due to calcite precipitation by bacteria spores and autogenous healing. Once the cracks are closed at the surface, it is expected that lower amounts of moisture penetrate into the matrix, which results in limited autogenous sealing in the concrete interior. Similar findings have been reported in past studies [5,42], in which regions close to the surface of cracked samples contained high amount of healing product, while limited amount of healing product (carbonate or products from further hydration or pozzolanic reaction) was generated at greater depths from surfaces. Although bacterial metabolism is

an active process within the concrete, generation of bio-carbonate and its effective transport distance to the crack site may be affected by reduction in the size, depth, and number of pore channels in the cementitious matrix with age.

Our past study on cement mortar with a combination of biocharimmobilized spores, SAP, and fiber showed 90-95% sealing in the case of relatively wide cracks (700-900 µm) [16]. However, in this study, lower sealing ratios (about 65%) were obtained in concrete with similar combinations after one cycle. This result is attributable to the difference in sample size, crack location, closure time, and curing condition, as well as the existence of coarse aggregates, which, as discussed, exhibit less self-healing. In the earlier case, crack closure was observed for a single through-crack at the middle of a $40 \times 40 \times 160$ mm prism over a period of 21 days under continuous moist curing, while, in this case, monitoring of surface cracks on a 100 mm (d) x 200 mm(h) samples was performed under wet-dry cycling for 14 days. A through crack offers better moisture distribution and a continuous transport channel for healing agent to the crack site, while surface cracks in cylinders may not offer a continuous pathway. Transport of healing agent (bacteria and substrate compounds) is more efficient in the case of smaller samples, because the transport distance is shorter than in the case of 100 mm(d) x 200 mm(h) cylinders. Continuous moisture supply over 21 days also improved crack filling by the autogenous healing mechanism (i.e., rehydration of cement grains) compared to only a 9-h period of moist curing each day in the present study over 14 days. This finding is supported by Luo et al. [32], who reported that water curing offered approximately 29% improvement in crack area repair rate compared to wet-dry cycles (12-h wet period) at 14-days.

3.4. Recovery of strength and elastic modulus

Fig. 6 (a) presents the compressive strength of concrete mixes that were healed after the first, second, and third cycles of damage. Although strength values are important for structural applications, the comparison of healing is incomplete without quantifying the percentage of strength regained with respect to the undamaged counterparts of each mix, because the difference in material combinations influence strength development. Thus, the recovery in strength (*RS*), presented in

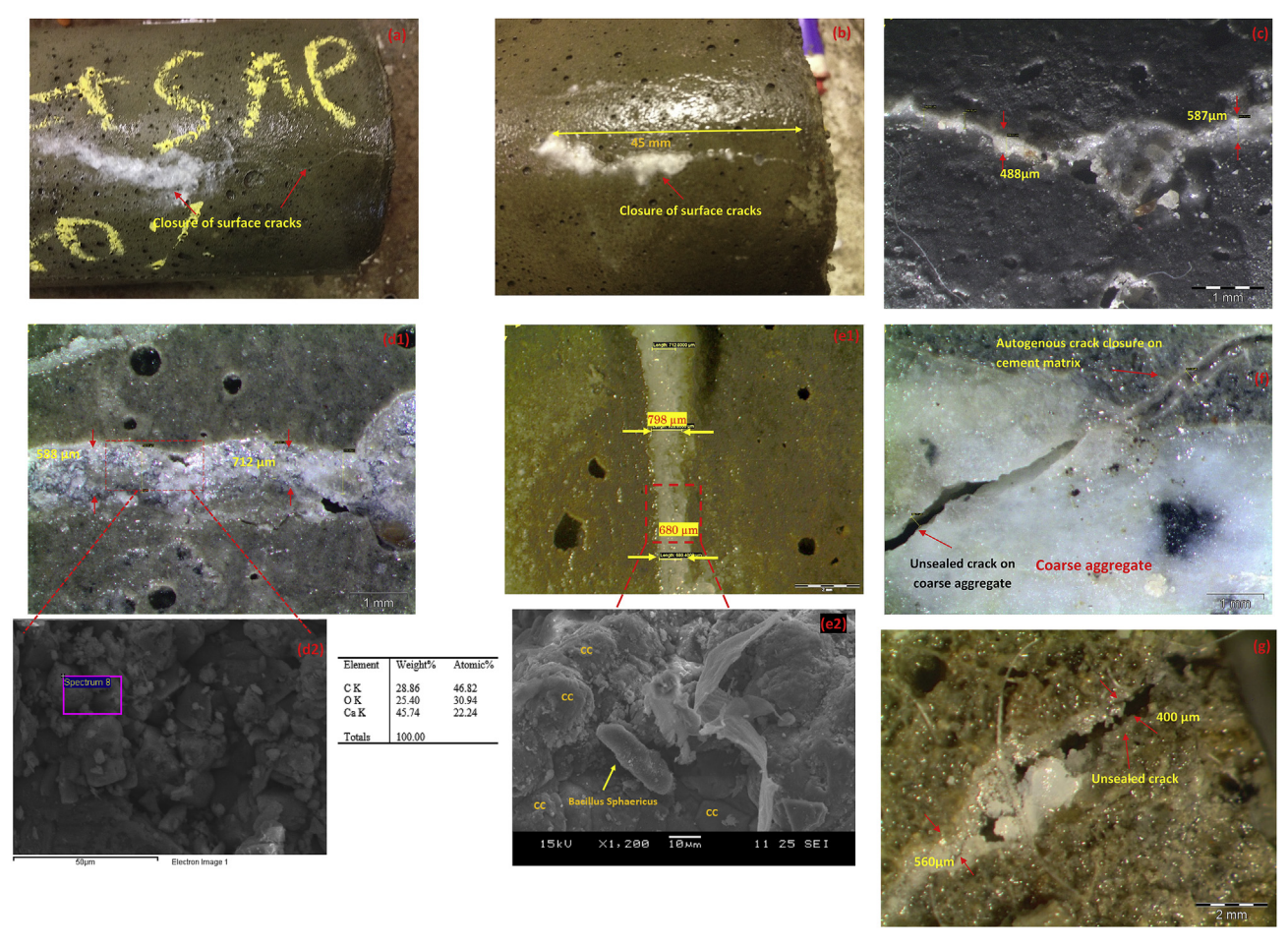


Fig. 5. (a) and (b) Filling of surface cracks on concrete cylinders in biochar-immobilized spore + SAP (A and B) samples after three damage-healing cycles, (c) Sealing of internal cracks in (BS-BC)-SAP-A + Fib samples after three damage-healing cycles, (d1) Sealing of internal cracks in (BS-BC)-SAP-B + Fib samples after three damage-healing cycles, (d2) SEM-EDS spectra of precipitated carbonate at the crack (e1) Complete crack sealing of surface crack of 680–800 μm in (BS-BC)+SAP-A + Fib samples after third healing cycle (e2) SEM micrograph of healing agent showing precipitated calcium carbonate crystals (CC) around a cell of Bacillus Sphaericus (f) Incomplete closure of cracks passing through coarse aggregate (g) Partially closed crack in concrete with biochar-immobilized spores, fiber and SAP-B.

Fig. 6(b), is calculated using Eq. (3).

$$RS = \frac{\sigma_H}{\sigma_U} \tag{3}$$

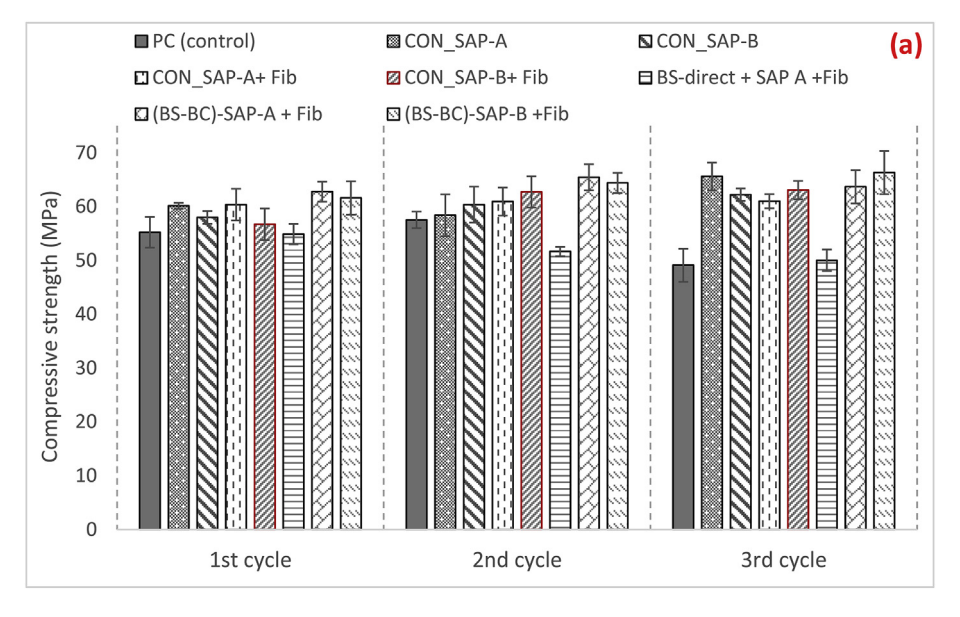
Where, σ_H and σ_U are the strength (MPa) of healed concrete and undamaged concrete after each healing cycle. Recovery of 1 or higher means complete healing, while a value < 1 would indicate partial healing with respect to the undamaged mix.

Plain concrete (control) showed similar compressive strength values after the first and second cycles of healing. The recovery in strength also shows a similar trend – 0.93 and 0.92 after the first and second healing cycle. This finding suggests that the strength in healed control concrete is not significantly impaired up to the second cycle of damage. Although loading induces cracks, compressive strength is not significantly affected by micro-cracking unless significant crack propagation has occurred. Secondly, at early stage there is a higher fraction of unhydrated particles and the water can penetrate within the sample easily, which can generate autogenous healing and contribute to strength recovery. However, after the third cycle, significant decreases in strength and recovery ratios are observed for plain concrete. While a strength reduction of 17.50% was observed, the corresponding recovery ratio dropped to 0.74 compared to 0.92 in the second cycle. This result is attributed to insufficient healing, which may be due to the propagation and coalescence of unsealed cracks inherited from the previous cycles of damage. Due to availability of water near the concrete surface and ongoing hydration, limited moisture is available within the interior

for crack sealing at later ages [5,43]. This finding implies that many cracks developed within the samples due to repeated damage would not be healed completely and that these cracks can propagate easily under further loading and affect the ultimate load carrying capacity.

The strength values of CON_SAP-A and CON_SAP-B after the first and second cycles of healing are statistically similar to that of healed plain concrete (p = 0.10 and 0.15 > 0.05, tested at 95% confidence interval). A similar trend is also observed for concrete with combination of SAP and fiber (CON_SAP-A + Fib and CON_SAP-B + Fib), which shows similar strength development and recovery ratios after healing as that of concrete containing only SAP. This result indicates that fiber hybridization did not play an important role in strength recovery, which is linked to the damage level (60%f) for samples at each cycle. At 60%f, it is expected that only discrete micro-cracks will originate in the matrix, which would not impair load carrying capacity of concrete. Therefore, addition of hybrid fibers does not significantly influence strength recovery compared to the unreinforced mix (containing only SAP), although, as will be discussed, fibers play an important role in recovery of permeability.

Zhong and Yao [43] reported that recovery of compressive strength after damage reduced significantly with age of concrete because of limited moisture penetration into the interior of the sample, which will limit the hydration of unhydrated cement particles. This result is also observed in this study, in which concrete with SAP showed higher strength recovery compared to the control after the third cycle. This result indicates the beneficial effects imparted by SAPs, which



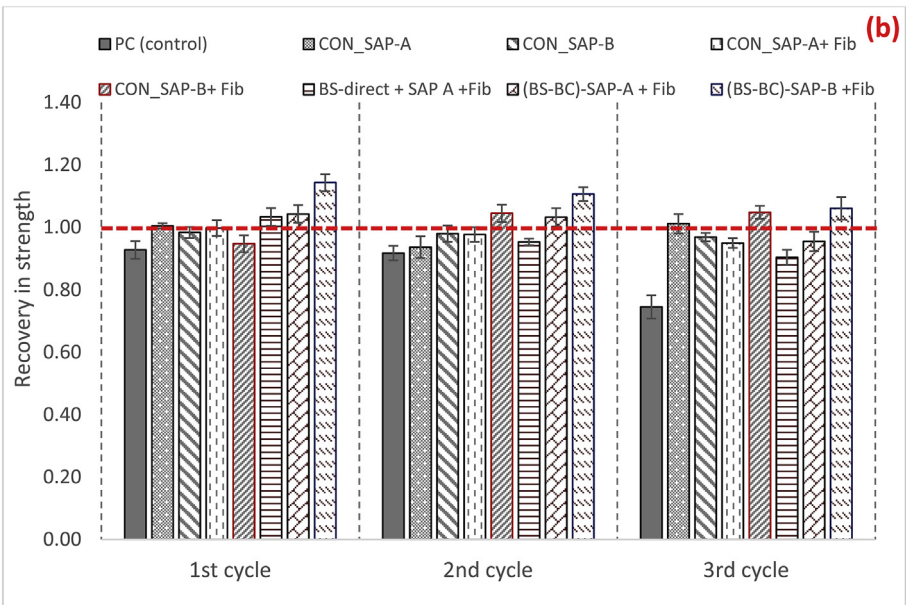


Fig. 6. (a) Compressive strength of concrete with different healing agents after first, second, and third healing cycle. (b) Recovery of compressive strength after first, second, and third healing cycle.

internally enhance hydration and contribute to continual strength development.

Although a safety factor of 1.50 (working load = 0.66 of design load) is used for structural concrete as per limit state design and reinforcement limits excessive deflection and cracking, it is important for the concrete to maintain its characteristic strength for structural integrity. Recovery of strength between 0.95 and 1.0 after 3 cycles of damage indicates that the combination of SAP and fiber can be a potential approach to maintain structural integrity under repeated loading.

Direct addition of bacteria (BS direct + SAP A + Fib) results in similar compressive strength as control mortar after first healing cycle. However, the strength is lower compared to concrete with SAP-A and fiber (CON_SAP-A + Fib), which means that directly added bacteria did not have significant influence on strength development after healing. Immobilization of bacteria in biochar with SAP and fiber show higher strength development after all cycles of healing compared to directly added spores. For example, after third cycle of healing, (BS-BC)-SAP-A + Fib show about 25% higher strength and 16% higher recovery

ratio than directly added spores. It implies that immobilization in biochar plays an important role in strength recovery after repeated healing. Besides offering protection to the bacteria spores, biochar particles may act as a filler and micro-reinforcement by resisting crack propagation and imparting ductile behavior to the cementitious matrix, as discussed in past studies [44–46].

After each healing cycle, (BS-BC)-SAP-A + Fib and (BS-BC - SAP-B + Fib show similar trends in strength development (Fig. 6(a)). However, in terms of recovery, (BS-BC) - SAP-B + Fib show consistently high recovery in strength compared to (BS-BC)-SAP-A + Fib (Fig. 6(b)) Similar behavior is shown by CON_SAP-B + Fib (without bacteria spores), which showed higher recovery in strength compared to CON_SAP-A + Fib. This result might be linked to higher moisture absorption capacity of SAP-B (300 g/g and 33 g/g of dry SAP in tap water and cement filtrate respectively, Table 3), which has a positive effect on recovery of mechanical strength. This finding means that higher amounts of moisture can be retained internally within the concrete matrix for supporting bacterial metabolism and autogenous healing. (BS-BC)-SAP-B + Fib shows an increase in strength after

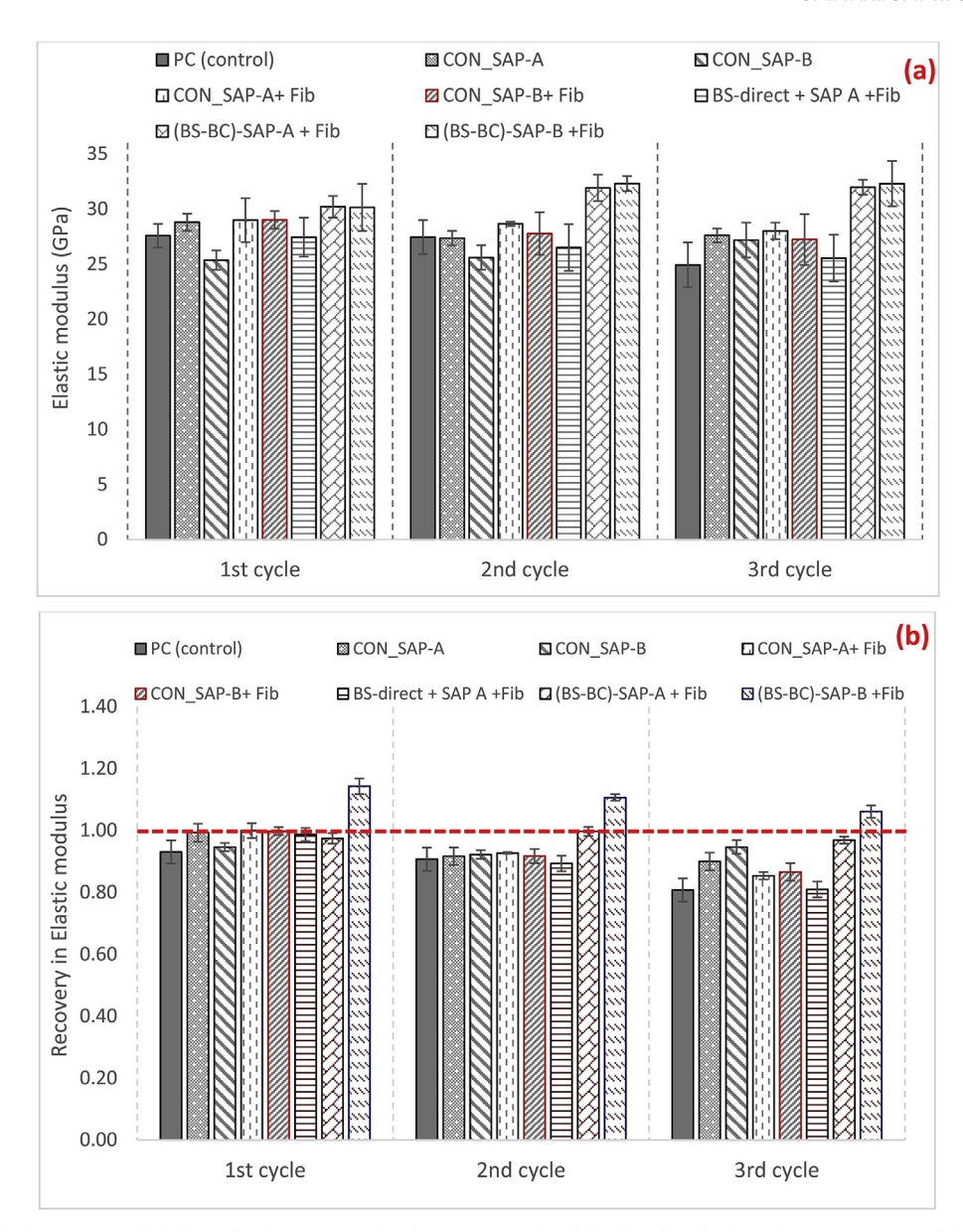


Fig. 7. (a) Elastic moduli of concrete with different healing agents after the first, second, and third cycle of healing (b) Recovery of modulus of elasticity of concrete after 1st, 2nd and 3rd cycle of healing.

each cycle of healing, which indicates that the internal hydration and precipitation of calcium carbonate compensates the strength loss caused by repeated loading.

Elastic modulus is more affected compared to strength by the weaker interfacial transition zone around fibers and aggregates in cementitious matrices due to the presence of micro-cracks and unhydrated particles [25]. While one can observe that mixes without biochar-immobilized bacteria spores show a reduction in elastic modulus values after each healing cycle, (BS-BC) - SAP -A + Fib and (BS-BC) - SAP -B + Fib show increases in elastic modulus from the first to second cycle of healing, after which it is maintained at a similar level after the third cycle (32 and 32.30 GPa) (Fig. 7(a)). It can be observed that concrete with biochar-immobilized spores, SAP, and fiber show higher recovery in elastic modulus after 3rd healing cycle compared to concrete with only SAP and fiber, although there was a slight reduction in recovery from second to third healing cycle (Fig. 7(b)). This might be attributed to remediation of weak zones including pores and microcracks within the concrete matrix by calcium carbonate crystals produced by biochar immobilized bacteria.

SEM micrographs at the fiber-matrix zone of healed (BS-BC)-SAP-

A + Fib and (BS-BC)-SAPB + Fib shows generation of rhombohedral carbonate crystals of size 2-20 µm (Fig. 8(a) and (b)), that wrap around the PVA fibers and cover the fiber-cement interfacial zone. Their presence suggests that the hydrophilic surface of PVA fiber also facilitates internal deposition of calcium carbonate crystals. Similar precipitation is also observed in the aggregate-paste zone in (BS-BC)-SAP-A + Fib mix (Fig. 8 (e)). The calcite crystals fill the pores and micro-cracks at the fiber-matrix interface and aggregate-paste interface, which remediate the relatively weak interfacial zones of concrete. Similar observation is reported by Sierra-Beltran et al. [47], who report that calcite precipitation at the fiber-matrix surface contributed to full recovery of flexural stress and deflection capacity (recovery ratio of 1.01 and 1.28 respectively) after healing at 56-day [47]. Besides calcite deposition at the interface, generation of healing product can also be seen inside internal cracks, bridged by fibers in (BS-BC)-SAP + Fib mixes (Fig. 8 (c)). A magnified image (Fig. 8 (d)) of the healing product show calcite crystals along with some hydration products. These crystals suggests that hydration and generation of bio-calcite may play an important role in sealing internal micro-cracks that contribute to restoration of original strength and elastic modulus of concrete after

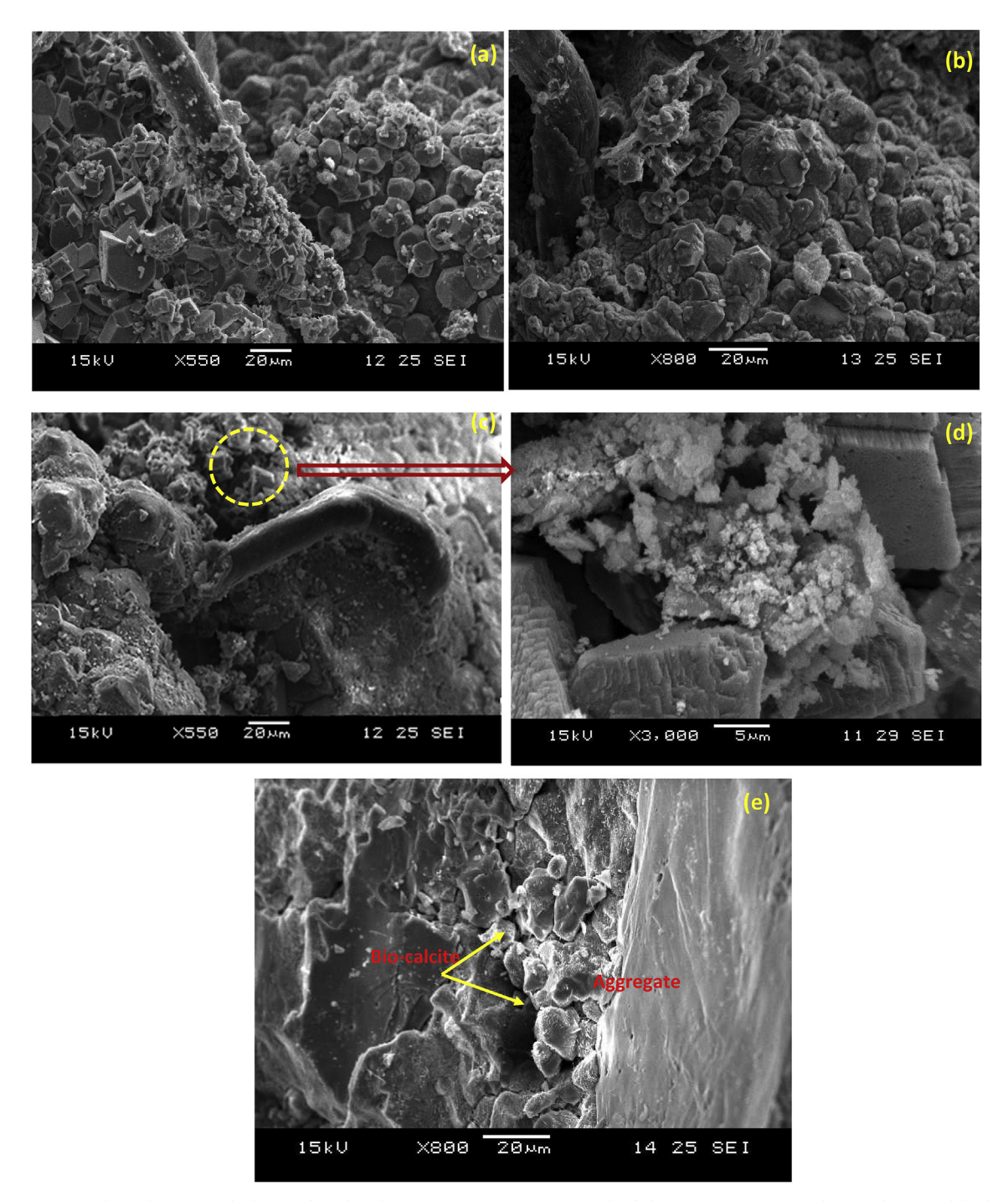


Fig. 8. (a) Wrapping of bio-calcite around fibers and at the fiber-cement matrix interface in healed (BS-BC) - SAP-A + Fib after the second healing cycle; (b) Precipitation of bio-calcite around the fiber-matrix interface in (BS-BC) - SAP-B + Fib; (c) Crack bridging and filling of cracks with calcite crystals; (d) Magnified image of healing product inside cracks in Fig. 11(c); (e) Calcite crystals at paste-aggregate interface.

healing.

3.5. Recovery of capillary absorption and water sorptivity

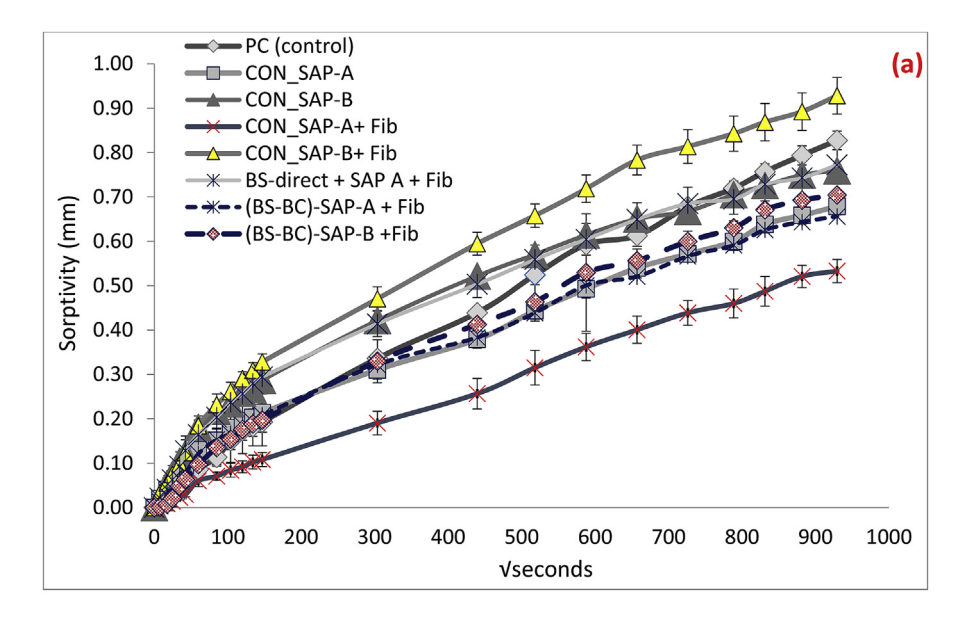
Recovery of permeability properties after self-healing is important to ensure long-term durability after damage events by preventing accelerated ingress of detrimental fluids (e.g., saltwater) into the matrix. Recovery of permeability (R_p) was quantified using equation (4):

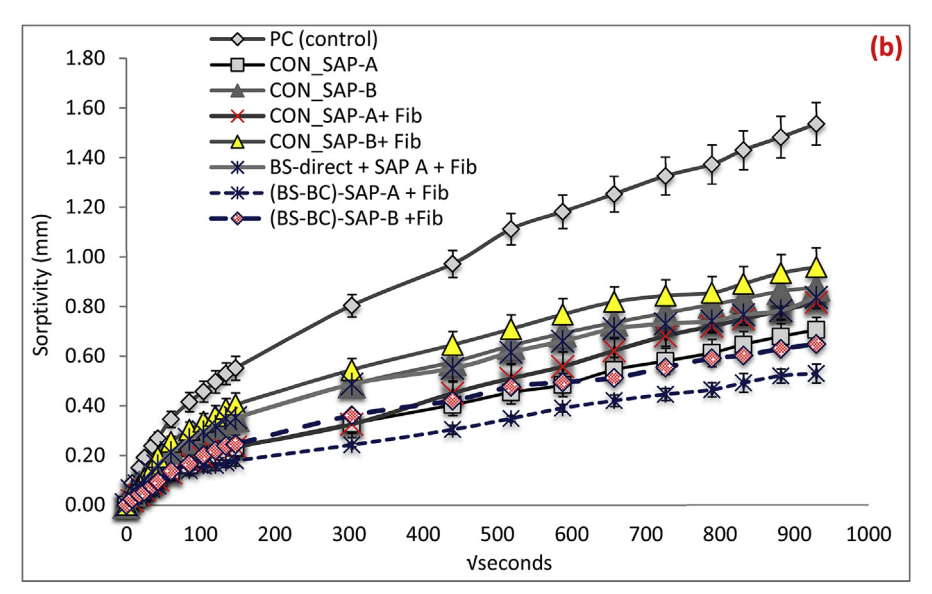
$$R_p = \frac{S_{ud}}{S_h} \tag{4}$$

Where, S_{ud} and S_h refer to sorptivity of undamaged concrete and healed

concrete respectively after each healing cycle. Similar to mechanical strength, a recovery ratio of 1 or greater corresponds to complete recovery, while a ratio of < 1 would indicate partial healing.

Capillary absorption of healed concrete mixes after the first, second, and third cycle of healing are shown in Fig. 9(a) and (b) and (c) respectively. Although water absorption is related to the original (undamaged) micro-structure of concrete, which varies with the mix composition (i.e., presence of SAP, biochar, etc.), comparison of total absorption is important to understand the permeability of each mix after healing. Initial and secondary coefficient of sorptivity (or rate of absorption) was used to calculate recovery of sorptivity after each cycle





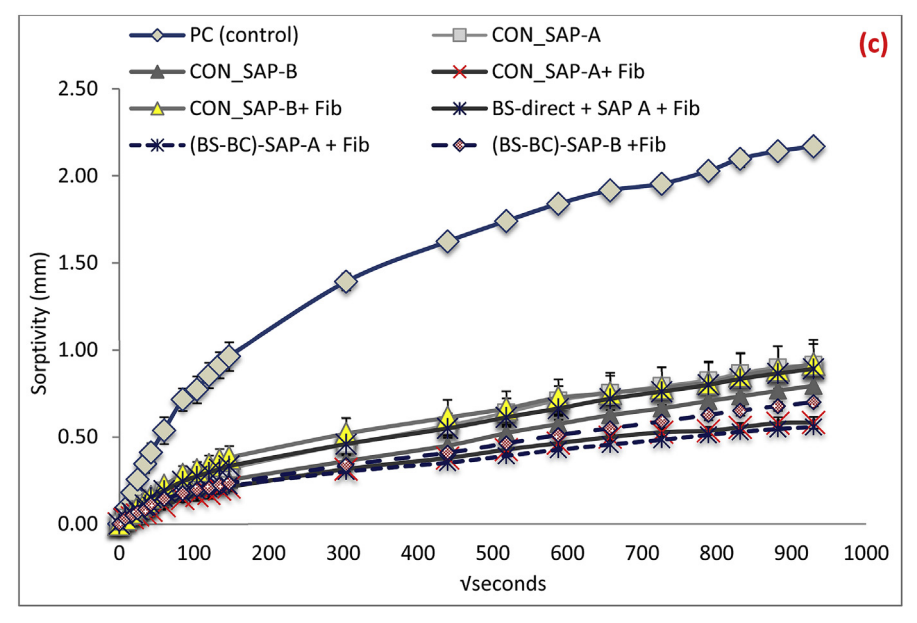


Fig. 9. Sorptivity of mixes after the (a) first, (b) second, and (c) third cycle of healing.

Table 4Recovery of initial and secondary coefficient of sorptivity after the first, second, and third healing cycle.

		ery of initiation			ery of secon	
	First cycle	Second cycle	Third cycle	First cycle	Second cycle	Third cycle
PC (control)	1.62	0.55	0.18	1.00	0.62	0.50
CON_SAP-A	1.35	1.07	0.41	1.31	0.85	0.60
CON_SAP-B	1.12	0.93	0.84	1.16	0.72	0.69
CON_SAP-A + Fib	1.89	0.91	0.36	0.93	0.94	0.92
CON_SAP-B + Fib	0.90	0.66	0.44	0.79	0.86	0.87
BS-direct + SAP A + Fib	0.75	0.72	0.66	1.23	1.15	0.63
(BS-BC)-SAP-A + Fib	1.08	1.02	0.98	1.00	1.08	0.86
(BS-BC)-SAP-B + Fib	1.11	1.09	0.81	1.03	0.73	0.68

of healing (Table 4). After the first cycle of healing, (BS-BC)-SAP A + Fib and (BS-BC)-SAP-B + Fib show 20% and 15% lower absorption compared to plain concrete (Fig. 9(a)). However, recovery of sorptivity is higher in plain concrete compared to concrete with directly added or immobilized bacteria along with SAP and fibers. This result may be linked to the closing of voids and existing micro-cracks due to applied stress below the threshold load level in case of plain concrete [48,49]. The threshold level is defined as the stress that induces significant cracking and results in an increase in bulk permeability. However, threshold level needs further investigation because there are varied findings regarding the threshold stress. Kermani [49], for example, reported that threshold value is between 40 and 50% of the peak stress under compression, while other studies [48,50] reported it to be in the range of 60%-80% peak stress. Addition of hybrid fibers increase the threshold value of stress and the cracking profile by introducing discrete narrower cracks rather than a few large cracks in the matrix [51]. It is reflected in highest recovery of initial sorptivity in CON SAP-A + Fib samples after first cycle of healing. However, the same was not witnessed in case of CON_SAP-B + Fib, which is possibly due to higher swelling in case of SAP-B compared to SAP-A, leading to formation of macro-voids in case of SAP-B mix. In the case of tap water (used for mixing concrete) and cement filtrate, SAP-B shows higher swelling compared to SAP-A, which is statistically significant at 95% confidence interval (p-value = 0.001 < 0.05). Under loading, the macro-voids lead to stress localization, which initiate cracking and contribute to higher water absorption compared to mix containing SAP-A and fiber. A

similar trend can be observed if recovery of CON_SAP-A and CON_SAP-B is compared—CON_SAP-A show 15% reduction in total absorption and higher recovery in initial and secondary sorptivity coefficient compared to CON SAP-B.

Direct addition of bacteria spores (BS direct+ SAP A + Fib) does not show significant reduction in water absorption compared to plain concrete after first damage-healing cycle. Compared to CON_SAP-A + Fib, concrete with directly added spores shows higher absorption and lower recovery in initial coefficient of sorptivity (Table 4). This result may be related to generation of additional pores in the cementitious paste due to addition of bio-substrates including yeast extracts and peptone [52].

The trend in sorptivity is altered after the second and third healing cycles, where the difference in total absorption by plain concrete and mixes containing healing agents (SAP, bacteria etc.) is larger. For example, (BS-BC)-SAP-A + Fib and (BS-BC) - SAP-B + Fib show 65% and 57% lower total absorption respectively compared to plain concrete after cycle 2, while the reduction is 75% and 68% respectively after the third healing cycle. While the recovery ratio of initial sorptivity, attributed to strong capillary suction by fine pores and micro-cracks, drops to 0.55 and 0.18 after the second and third cycle of healing, respectively, mixes with biochar-immobilized spores offer recovery of 0.98 and 0.81 after the third healing cycle, respectively.

A similar trend is observed in the case of capillary rise of water, which was quantified by measuring the depth of water front from the water-exposed face of sorptivity samples. These measurements were taken at identical locations on the of 100 mm (d) x 200 mm(h) cylinders. Plain concrete shows a 60-70% increase in capillary rise after the third healing cycle compared to that after the first cycle. Comparing Fig. 10 (a1) and (a2), one can observe that water has penetrated throughout the healed plain concrete after the third cycle, while the rise was lower after the first healing cycle. Unsealed micro-cracks open path for transport of moisture into the hardened sample, hence increasing the transport distance from the point of entry, CON SAP-A + Fib also exhibit a significant change in capillary rise from the first to the third healing cycle (Fig. 10 (b1) and (b2)). However, for (BS-BC)-SAP-A + Fib, the increase in capillary rise was limited to only 20-25%, which can be observed from a small change in depth of water front from Fig. 10 (c1) (cycle 1 of healing) to Fig. 10(c2) (cycle 3 of healing). Recovery in initial sorptivity coefficient of (BS-BC)-SAP-A + Fib is higher than CON_SAP-A + Fib after the second and third healing cycle, although the total absorption values are similar. In the case of (BS-BC)-SAP-B + Fib, the overall recovery is higher, and total absorption values

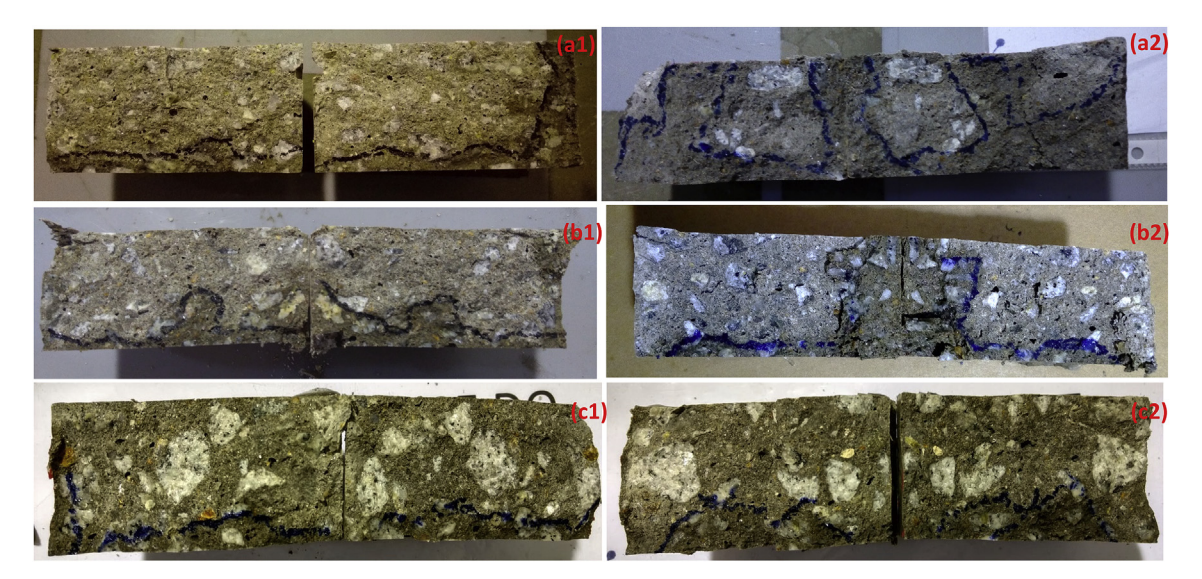


Fig. 10. Capillary rise during the sorptivity test after the first healing cycle in (a1) Plain concrete (b1) CON_SAP-A + Fib (c1) (BS-BC) - SAP-A + Fib and after the third healing cycle in (a2) Plain concrete (b2) CON_SAP-A + Fib (c2) (BS-BC) - SAP-A + Fib.

after the third cycle are reduced by 22.50% and 17% compared to its counterpart with only SAP-B and fiber. These results indicate that there is a lower connectivity of cracked network for transport of moisture in healed (BS-BC) -SAP-(A and B) + Fib mix compared to plain concrete and CON_SAP (A or B) + Fib mixes. This result can be attributed to the internal sealing of micro-cracks and densification of fiber-matrix (Fig. 8(a) and (b)) and aggregate-matrix interfaces (Fig. 8(e)), which reduces capillary suction and rise of fluid into the healed concrete. Moreover, a significant fraction (90%) of biochar particles are finer than cement (Fig. 1), which implies that biochar may have micro-filler effect. Micro-fillers can block paths for moisture transport by filling pore spaces between cement grains or cement-aggregate interfaces.

The threshold value and change in permeability of plain concrete depends on loading history. If plain concrete is previously damaged, such as after the first loading cycle, the threshold load for the second and third loading cycle would be lower compared to the initial level [53]. This reduction is likely due to a network of unsealed micro-cracks, which leads to a rapid increase in permeability [53,54]. While plain concrete shows an increase in sorptivity from the second to the third cycle (about 33% increase), concrete with biochar-immobilized bacteria shows a smaller shift in absorption under repeated loading (for example, 4% increase for (BS-BC) -SAP A + Fib mix from cycle 2 to cycle 3). This result is attributable to the sealing of internal cracks by bacterial calcite, as evidenced by SEM imaging. Fig. 11(a)-(c) show that cracks between 100 and 150 µm are filled with calcite crystal depositions that are rhombohedral in shape and approximately $10-70\,\mu m$ in size—calcite depositions typical of the morphology produced by Bacillus Sphaericus in concrete [55,56]. Biogenic calcite precipitation results in refinement of the porosity generated by voids and micro-cracks in damaged concrete, resulting in lower permeability in samples with immobilized bacteria. Recovery of initial and secondary coefficient of sorptivity in the case of (BS-BC) - SAP-B + Fib after the third healing cycle is lower compared to that of (BS-BC)-SAP-A + Fib. A possible hypothesis for this finding is that the voids created by desorption of SAP-B are relatively large due to its higher average particle size and higher swelling capacity compared to SAP-A, which cannot be completely sealed by bacterial calcite. For example, although generation of calcite crystals is observed around an internal void of size 100 μ m in (BS-BC)-SAP-B + Fib at 56-day (Fig. 11(d)), a large part of the void remains unfilled. Such macro-pores may connect to smaller pores, resulting in higher open porosity and permeability of the cementitious matrix [25].

Table 5 summarizes the summarize the distinction between autogenous healing (plain concrete and concrete containing, SAP/fiber), crack filling and healing by MICP in directly added spores, and biochar immobilized spores respectively.

4. Scope of further research

Although this study suggests that biochar-immobilized bacteria along with SAP improved self-healing efficiency, further research is necessary to investigate effect of SAP addition on cyclic freeze-thaw damage of concrete. Mechtcherine et al. [57] conducted extensive test on freeze-thaw resistance of SAP concrete with two SAP types: SAP 1 (particle size between 50 and 600 μm) and SAP 2 (fparticle size between 20 and 200 μm). Both SAPs had comparable swelling capacity of 33–35 g/g. The test results showed that at constant water-binder ratio of 0.45 (without additional water), concrete with both SAP 1 and SAP 2 showed 69% and 77% lower scaling (g/m²) compared to control concrete after 28 cycles of freeze-thaw test with deicing salts. It is reported that the resistance to freeze-thaw damage due to addition of SAP is influenced by dosage, particle size , and its fluid retention capacity

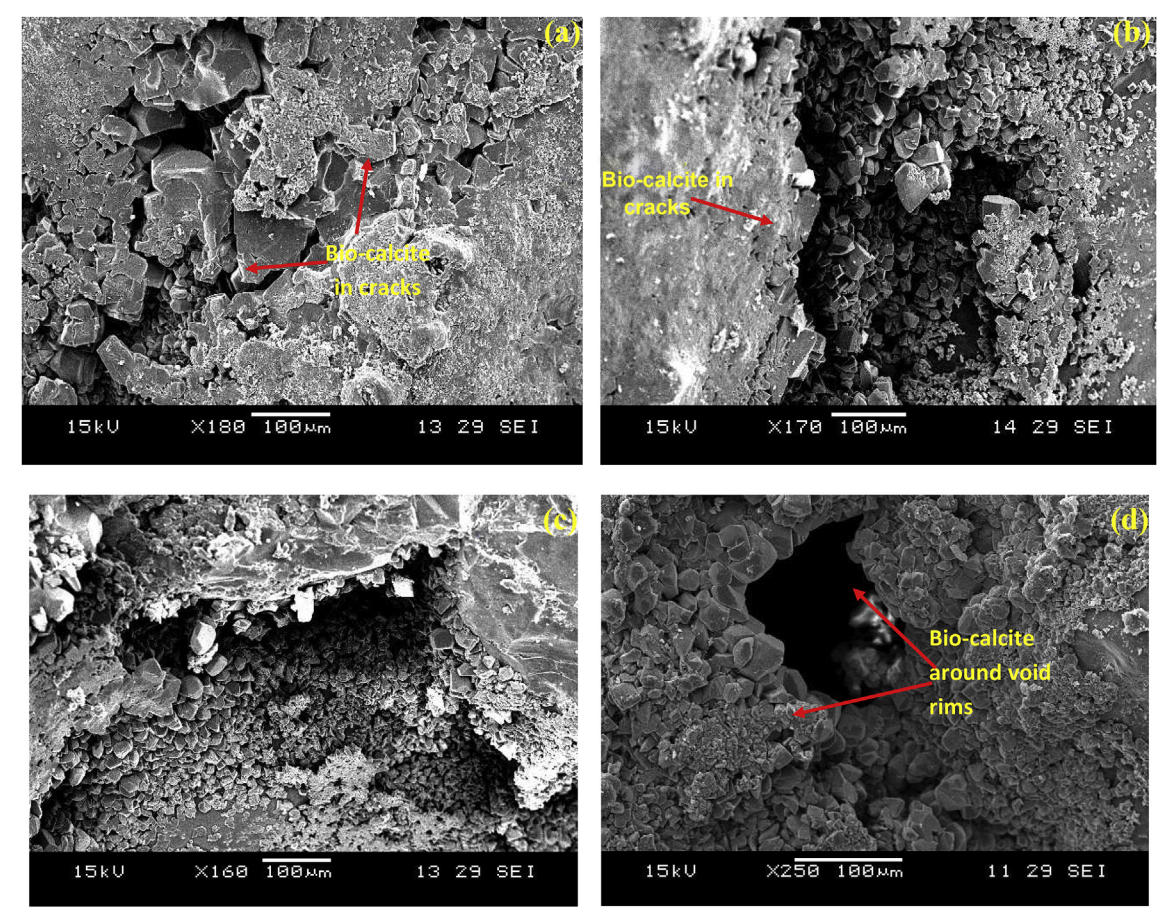


Fig. 11. Deposition of bio-calcite in (a) and (b) cracks of (BS-BC)-SAP A + Fib (c) in cracks of (BS-BC) - SAP-B + Fib (d) Voids of (BS-BC) - SAP-B + Fib.

Summary of crack filling and healing effectiveness of three strategies - autogenous healing by SAP/fiber, directly added spores and biochar immobilized spores.

	o o-	o	J	I_	
		Autogenous healing (Plain concrete)	Autogenous healing (with SAP and SAP + fiber)	Crack filling and healing by directly added bacteria spores with SAP and fiber	Crack filling and healing by biochar immobilized bacteria with SAP and fiber
	Crack filling	No or very minimal sealing of cracks above 300 µm in all cycles of testing Efficacy of sealing reduce with number of cycles (or age of concrete)	 Crack filling ratio of 70-80% for narrow cracks (200-400 µm) due to SAP swelling upon exposure to water and contribution to hydration Drastic reduction in crack filling ratio to 10-18% for wide cracks (> 550 µm) 	 50–60% crack filling observed for relatively wide micro-cracks (400–700 µm) after first healing cycle Filling effectiveness reduced to only 18–30% for 400–700 µm cracks after third cycle due to reduced bacterial activity 	 35-40% crack filling for wide micro-cracks (550-700 µm) after third healing cycle. No significant reduction in filling effectivenes from first to third cycle for cracks width between 400 µm and 800 µm
Healing effectiveness	Recovery of mechanical properties	Reduction in strength and recovery of elastic modulus and strength from cycle 1 to cycle 3	 Reduction in crack filling effectiveness from cycle 1 to cycle 3 of healing Recovery of elastic modulus of 80–90% after third healing cycle 	 Recovery of 80% and 90% for compressive strength and elastic modulus after third healing cycle 	 Recovery of elastic modulus and compressive strength by 96–100% after third healing cycle
	Recovery of sorptivity	Only 74% and 80% recovery in strength and elastic modulus achieved after cycle 3. Only 18% and 50% recovery in initial and secondary sopptivity after cycle 3	• Complete recovery of initial sorptivity after cycle 1. However, drastic reduction to recovery ratio of 41-84% is observed after third healing cycle	 Recovery of initial and secondary sorptivity reduced to 66% and 63% after cycle 3 compared to 75% and 123% respectively after first healing cycle 	 Recovery of initial and secondary sorptivity by 81–98% and secondary sorptivity by 86% and 68% with SAP-A and SAP-B respectively.

[57,58]. Craeye et al. [58] reported that high spacing factor of voids in relative large size SAP particles (560 μ m in their study) may not be effective in resisting freeze-thaw damage.

Although SAP contributes to self-healing of pre-cracked concrete in general [12,59], there is a dearth of research in role of SAP in self-healing of cracks in concrete subject to freeze-thaw damage. Therefore, further research must be conducted to understand how SAP of certain type, particle size, and swelling capacity (for instance, SAP-A and SAP-B used in this study) may contribute to blocking and crack filling in undamaged or pre-cracked concrete subject to freeze-thaw cycles. It would contribute to optimization of dosage and particle size of these SAP types to complement bio-based self-healing in concrete especially in regions with continental and temperate climates.

The efficacy of biochar-bacteria enhanced self-healing in actual environment should be investigated. It is important to look into the possibility of developing genetically modified bacteria, which should be economic and produce carbonate at a faster rate for rapid filling of cracks. These studies should aim to enhance the service life, reduce cost, and evaluate the environmental and social benefits in detail.

5. Conclusion

This study investigated the self-healing behavior of concrete with biochar-immobilized spores, SAP, and fibers under three cyclic damage and healing cycles. Filling of cracks and recovery of mechanical and permeability properties was compared with that achieved by autogenous healing in control and concrete containing superabsorbent polymer and fiber. The following conclusions can be drawn based on this experimental investigation:

- a) Addition of SAP and fiber (CON_SAP + Fib) lead to improved autogenous healing compared to plain concrete by sustaining hydration, swelling, and precipitation of calcium carbonate, that block narrow micro-cracks. However, the efficacy of crack-filling by SAP (or combination of SAP and fiber) is found to be low for relatively wide micro-cracks (> 500 μm). Regardless of SAP type, noticeable reduction in crack-filling ability and recovery of permeability is also observed from first healing cycle to third healing cycle in concrete with combination of SAP and fiber.
- b) Comparison of crack-filling for three healing cycles suggests significant improvement in surface crack-sealing by combination of SAP with biochar-immobilized spores compared to plain concrete and concrete with only SAP and fibers. The results suggest that, although addition of SAP and fiber offer improved crack filling than plain concrete, introduction of bacteria, directly or in immobilized form, boost crack filling efficiency, especially for relatively wide cracks. This enhanced performance is due to formation of biogenic calcium carbonate that leads to an appreciable repeated filling of relatively wide micro-cracks (between 500 and 800 μm). Bacteria in biochar—as an immobilized material response mechanism—maintains crack filling efficacy over three cycles of healing, which was evident from a lower reduction in filling ratio in concrete with biochar immobilized spore compared to directly added spores.
- c) Higher strength after multiple healing and recovery in compressive strength and elastic modulus can be achieved by combination of biochar immobilized bacteria, SAP and hybrid fiber compared to control and mix with only SAP and fiber. The property recovery is due sealing of internal cracks and densification of fiber-paste and aggregate-paste interface zone by microbial induced calcite precipitation.
- d) Although direct addition of bacteria together with SAP and fiber show higher recovery of permeability than plain concrete after third healing cycle, the efficacy decreased with number of cycles (or age of concrete). Use of biochar as a carrier for bacteria spores contributes to lower permeability levels and higher recovery of sorptivity after three damage-healing cycles compared to concrete with

directly added spores. Fine particle size of SAP is found to be more conducive to recovery of permeability of self-healing compared to coarser particles with higher swelling capacity.

In summary, the findings from this study suggest that the proposed material combination of biochar immobilized bacteria, SAP, and fiber can potentially self-heal micro-cracks and retain material properties after repeated damage. This suggests that application of the proposed material can reduce repair cost and extend the service life of concrete infrastructure. Future research necessitates investigating the cost-effective production of bacterial cultures and utilization of other potential feedstocks for biochar, which are necessary to maximize the commercial viability of self-healing fiber-reinforced concrete.

Acknowledgement of funding

The authors would like to thank the Ministry of Education, Singapore, for providing the Academic Research Fund (tier-1) (R-296-000-163-112) to support this work.

Appendix A. Supplementary data

Supplementary data to this article can be found online at https://doi.org/10.1016/j.cemconcomp.2019.03.017.

References

- G. Souradeep, H.W. Kua, Encapsulation technology and techniques in self-healing concrete, J. Mater. Civ. Eng. 28 (12) (2016) 04016165.
- [2] K. Van Breugel, Is there a market for self-healing cement-based materials, Proceedings of the First International Conference on Self-Healing Materials Noordwijk Aan Zee, The Netherlands, 2007.
- [3] K. Van Tittelboom, N. De Belie, D. Van Loo, P. Jacobs, Self-healing efficiency of cementitious materials containing tubular capsules filled with healing agent, Cement Concr. Compos. 33 (4) (2011) 497–505.
- [4] T.D.P. Thao, T.J.S. Johnson, Q.S. Tong, P.S. Dai, Implementation of self-healing in concrete–proof of concept, IES J. Part A Civ. Struct. Eng. 2 (2) (2009) 116–125.
- [5] D. Snoeck, N. De Belie, Repeated autogenous healing in strain-hardening cementitious composites by using superabsorbent polymers, J. Mater. Civ. Eng. 28 (1) (2015) 04015086.
- [6] A. Mignon, G.-J. Graulus, D. Snoeck, J. Martins, N. De Belie, P. Dubruel, et al., pH-sensitive superabsorbent polymers: a potential candidate material for self-healing concrete, J. Mater. Sci. 50 (2) (2015) 970–979.
- [7] D. Snoeck, P. Van den Heede, T. Van Mullem, N. De Belie, Water penetration through cracks in self-healing cementitious materials with superabsorbent polymers studied by neutron radiography, Cement Concr. Res. 113 (2018) 86–98.
- [8] J. Wang, A. Mignon, G. Trenson, S. Van Vlierberghe, N. Boon, N. De Belie, A chitosan based pH-responsive hydrogel for encapsulation of bacteria for self-sealing concrete, Cement Concr. Compos. 93 (2018) 309–322.
- [9] F.L. Buchholz, A.T. Graham, Modern Superabsorbent Polymer Technology, John! Wiley & Sons, Inc, 605 Third Ave, New York, NY 10016, USA, 1998 1998 279.
- [10] J. Wang, A. Mignon, D. Snoeck, V. Wiktor, S. Van Vliergerghe, N. Boon, et al., Application of modified-alginate encapsulated carbonate producing bacteria in concrete: a promising strategy for crack self-healing, Front. Microbiol. 6 (2015) 1088.
- [11] D. Homma, H. Mihashi, T. Nishiwaki, Self-healing capability of fibre reinforced cementitious composites, J. Adv. Concr. Technol. 7 (2) (2009) 217–228.
- [12] D. Snoeck, K. Van Tittelboom, S. Steuperaert, P. Dubruel, N. De Belie, Self-healing cementitious materials by the combination of microfibres and superabsorbent polymers, J. Intell. Mater. Syst. Struct. 25 (1) (2014) 13–24.
- [13] W. Yao, J. Li, K. Wu, Mechanical properties of hybrid fiber-reinforced concrete at low fiber volume fraction, Cement Concr. Res. 33 (1) (2003) 27–30.
- [14] J.S. Lawler, D. Zampini, S.P. Shah, Microfiber and macrofiber hybrid fiber-reinforced concrete, J. Mater. Civ. Eng. 17 (5) (2005) 595–604.
- [15] S. Bhaskar, K.M.A. Hossain, M. Lachemi, G. Wolfaardt, M.O. Kroukamp, Effect of self-healing on strength and durability of zeolite-immobilized bacterial cementitious mortar composites, Cement Concr. Compos. 82 (2017) 23–33.
- [16] S. Gupta, H.W. Kua, S. Dai Pang, Healing cement mortar by immobilization of bacteria in biochar: an integrated approach of self-healing and carbon sequestration, Cement Concr. Compos. 86 (2018) 238–254.
- [17] J. Lehmann, M.C. Rillig, J. Thies, C.A. Masiello, W.C. Hockaday, D. Crowley, Biochar effects on soil biota—a review, Soil Biol. Biochem. 43 (9) (2011) 1812–1836.
- [18] J.E. Thies, M.C. Rillig, Characteristics of biochar: biological properties. Biochar for environmental management, Sci. Technol. (2009) 85–105.
- [19] NEA, Environmental Protection Division Annual Report, 2015/2016, Singapore National Environment Agency, Singapore, 2015, p. 2015.
- [20] R.B. Tan, H.H. Khoo, Impact assessment of waste management options in Singapore,

- J. Air Waste Manag. Assoc. 56 (3) (2006) 244-254.
- [21] F.F. Udoeyo, H. Inyang, D.T. Young, E.E. Oparadu, Potential of wood waste ash as an additive in concrete, J. Mater. Civ. Eng. 18 (4) (2006) 605–611.
- [22] K.G. Roberts, B.A. Gloy, S. Joseph, N.R. Scott, J. Lehmann, Life cycle assessment of biochar systems: estimating the energetic, economic, and climate change potential, Environ. Sci. Technol. 44 (2) (2009) 827–833.
- [23] D. Woolf, J.E. Amonette, F.A. Street-Perrott, J. Lehmann, S. Joseph, Sustainable biochar to mitigate global climate change, Nat. Commun. 1 (2010) 56.
- [24] S. Gupta, H.W. Kua, C.Y. Low, Use of biochar as carbon sequestering additive in cement mortar, Cement Concr. Compos. 87 (2017) 110–129.
- [25] S. Mindess, J.F. Young, D. Darwin, Concrete, Prentice Hall, Upper Saddle River, N.J.U.S.A. 2003.
- [26] A.N. Aday, J. Osio-Norgaard, K.E. Foster, W.V. Srubar, Carrageenan-based superabsorbent biopolymers mitigate autogenous shrinkage in ordinary portland cement, Mater. Struct. 51 (2) (2018) 37.
- [27] H. Hosseinzadeh, A. Pourjavadi, G. Mahdavinia, M. Zohuriaan-Mehr, Modified carrageenan. 1. H-CarragPAM, a novel biopolymer-based superabsorbent hydrogel, J. Bioact. Compat Polym. 20 (5) (2005) 475–490.
- [28] A. Pourjavadi, S.M. Fakoorpoor, P. Hosseini, A. Khaloo, Interactions between superabsorbent polymers and cement-based composites incorporating colloidal silica nanoparticles, Cement Concr. Compos. 37 (2013) 196–204.
- [29] A. Pourjavadi, A. Harzandi, H. Hosseinzadeh, Modified carrageenan 3. Synthesis of a novel polysaccharide-based superabsorbent hydrogel via graft copolymerization of acrylic acid onto kappa-carrageenan in air, Eur. Polym. J. 40 (7) (2004) 1363–1370.
- [30] S. Gupta, H.W. Kua, Effect of Biochar on Mechanical and Permeability Properties of Concrete Exposed to Elevated Temperature, National University of Singapore, 2018.
- [31] J. Lawler, T. Wilhelm, D. Zampini, S.P. Shah, Fracture processes of hybrid fiberreinforced mortar, Mater. Struct. 36 (3) (2003) 197–208.
- [32] M. Luo, C-x Qian, R-y Li, Factors affecting crack repairing capacity of bacteria-based self-healing concrete, Constr. Build. Mater. 87 (2015) 1–7.
- [33] W. Li, Z. Jiang, Z. Yang, N. Zhao, W. Yuan, Self-healing efficiency of cementitious materials containing microcapsules filled with healing adhesive: mechanical restoration and healing process monitored by water absorption, PLoS One 8 (11) (2013) e81616.
- [34] D. Snoeck, S. Steuperaert, K. Van Tittelboom, P. Dubruel, N. De Belie, Visualization of water penetration in cementitious materials with superabsorbent polymers by means of neutron radiography, Cement Concr. Res. 42 (8) (2012) 1113–1121.
- [35] P.J.M. Monteiro, P.K. Mehta, CONCRETE: Microstructure, Properties, and Materials. (2009).
- [36] ASTM, ASTM C39/39b: Standard Test Method for Compressive Strength of Cylindrical Concrete Specimens, ASTM International, West Conshohocken, Pennsylvania, United States, 2017.
- [37] ASTM, ASTM C469: Standard Test Method for Static Modulus of Elasticity and Poisson's Ratio of Concrete in Compression, ASTM International., West Conshohocken, PAJJSA, 2014.
- [38] ASTM, ASTM C1585-13: Standard Test Method for Measurement of Rate of Absorption of Water by Hydraulic-Cement Concretes, ASTM, West Conshohocken, Pennsylvania, United States, 2013.
- [39] P.H. Borges, J.O. Costa, N.B. Milestone, C.J. Lynsdale, R.E. Streatfield, Carbonation of CH and C–S–H in composite cement pastes containing high amounts of BFS, Cement Concr. Res. 40 (2) (2010) 284–292.
- [40] W.A.W.A.K. Ghani, A. Mohd, G. da Silva, R.T. Bachmann, Y.H. Taufiq-Yap, U. Rashid, et al., Biochar production from waste rubber-wood-sawdust and its potential use in C sequestration: chemical and physical characterization, Ind. Crops Prod. 44 (2013) 18–24.
- [41] S. Kara, C. Tamerler, Ö. Pekcan, Cation effects on swelling of κ -carrageenan: a photon transmission study, Biopolymers: Orig. Res. Biomol. 70 (2) (2003) 240–251.
- [42] S. Fan, M. Li, X-ray computed microtomography of three-dimensional microcracks and self-healing in engineered cementitious composites, Smart Mater. Struct. 24 (1) (2014) 015021.
- [43] W. Zhong, W. Yao, Influence of damage degree on self-healing of concrete, Constr. Build. Mater. 22 (6) (2008) 1137–1142.
- [44] S. Ahmad, R.A. Khushnood, P. Jagdale, J.-M. Tulliani, G.A. Ferro, High performance self-consolidating cementitious composites by using micro carbonized bamboo particles, Mater. Des. 76 (2015) 223–229.
- [45] S. Gupta, H.W. Kua, C.Y. Low, Use of biochar as carbon sequestering additive in cement mortar, Cement Concr. Compos. 87 (2017) 110–129.
- [46] R.A. Khushnood, S. Ahmad, L. Restuccia, C. Spoto, P. Jagdale, J.-M. Tulliani, et al., Carbonized nano/microparticles for enhanced mechanical properties and electromagnetic interference shielding of cementitious materials, Front. Struct. Civ. Eng. 10 (2) (2016) 209–213.
- [47] M.G. Sierra-Beltran, H. Jonkers, E. Schlangen, Characterization of sustainable biobased mortar for concrete repair, Constr. Build. Mater. 67 (2014) 344–352.
- [48] M. Choinska, A. Khelidj, G. Chatzigeorgiou, G. Pijaudier-Cabot, Effects and interactions of temperature and stress-level related damage on permeability of concrete, Cement Concr. Res. 37 (1) (2007) 79–88.
- [49] A. Kermani, Permeability of stressed concrete: steady-state method of measuring permeability of hardened concrete studies in relation to the change in structure of concrete under various short-term stress levels, Build. Res. Inf. 19 (6) (1991) 360–366.
- [50] N. Hearn, G. Lok, Measurement of permeability under uniaxial compression-A test method, ACI Mater. J. 95 (1998) 691–694.
- [51] N. Banthia, A. Bhargava, Permeability of stressed concrete and role of fiber reinforcement, Mater. J. 104 (1) (2007) 70–76.
- [52] Erşan YÇ, F.B. Da Silva, N. Boon, W. Verstraete, N. De Belie, Screening of bacteria

- and concrete compatible protection materials, Constr. Build. Mater. 88 (2015) 196–203.
- [53] N. Banthia, A. Biparva, S. Mindess, Permeability of concrete under stress, Cement Concr. Res. 35 (9) (2005) 1651–1655.
- [54] M. Saito, H. Ishimori, Chloride permeability of concrete under static and repeated compressive loading, Cement Concr. Res. 25 (4) (1995) 803–808.
- [55] J. Wang, K. Van Tittelboom, N. De Belie, W. Verstraete, Use of silica gel or polyurethane immobilized bacteria for self-healing concrete, Constr. Build. Mater. 26 (1) (2012) 532–540.
- [56] J. Wang, H. Soens, W. Verstraete, N. De Belie, Self-healing concrete by use of
- microencapsulated bacterial spores, Cement Concr. Res. 56 (2014) 139-152.
- [57] V. Mechtcherine, C. Schroefl, M. Wyrzykowski, M. Gorges, P. Lura, D. Cusson, et al., Effect of superabsorbent polymers (SAP) on the freeze—thaw resistance of concrete: results of a RILEM interlaboratory study, Mater. Struct. 50 (1) (2017) 14.
- [58] B. Craeye, G. Cockaerts, P. Kara De Maeijer, Improving freeze–thaw resistance of concrete road infrastructure by means of superabsorbent polymers, Infrastructures 3 (1) (2018) 4.
- [59] H. Lee, H. Wong, N. Buenfeld, Potential of superabsorbent polymer for self-sealing cracks in concrete, Adv. Appl. Ceram. 109 (5) (2010) 296–302.